# NASA TECHNICAL MEMORANDUM

NASA TM-82462



# LAGRANGIAN LEAST-SQUARES PREDICTION OF SOLAR ACTIVITY

By Robert L. Holland, C. A. Rhodes, and Harold C. Euler, Jr.
Space Sciences Laboratory

April 1982


NASA

*George C. Marshall Space Flight Center*
*Marshall Space Flight Center, Alabama*

TECHNICAL REPORT STANDARD TITLE PAGE

| 1. REPORT NO. | 2. GOVERNMENT ACCESSION NO. | 3. RECIPIENT'S CATALOG NO. |
|---|---|---|
| NASA TM- 82462 | | |

| 4. TITLE AND SUBTITLE | 5. REPORT DATE |
|---|---|
| Lagrangian Least-Squares Prediction of Solar Activity | April 1982 |
| | 6. PERFORMING ORGANIZATION CODE |

| 7. AUTHOR(S) | 8. PERFORMING ORGANIZATION REPORT # |
|---|---|
| Robert L. Holland, C.A. Rhodes,* and Harold C. Euler, Jr. | |

| 9. PERFORMING ORGANIZATION NAME AND ADDRESS | 10. WORK UNIT NO. |
|---|---|
| George C. Marshall Space Flight Center<br>Marshall Space Flight Center, Alabama 35812 | 11. CONTRACT OR GRANT NO. |
| | 13. TYPE OF REPORT & PERIOD COVERED |
| 12. SPONSORING AGENCY NAME AND ADDRESS | Technical Memorandum |
| National Aeronautics and Space Administration<br>Washington, D.C. 20546 | 14. SPONSORING AGENCY CODE |

15. SUPPLEMENTARY NOTES

Prepared by Space Sciences Laboratory, Science and Engineering Directorate, NASA/MSFC

* Computer Sciences Corporation, Huntsville, Alabama

16. ABSTRACT

This report presents the results of comparison studies on various applications of statistical prediction methods for short-term (months) and long-term (years) forecasting of solar activity. The comparisons indicate that better predictions, in a chi-square sense, are possible by "lining up" the maximum (or minimums, or both) by cycle number. Evidence is also presented to support the existence of an aperiodic variation in the periods as well as the amplitudes.

| 17. KEY WORDS | 18. DISTRIBUTION STATEMENT |
|---|---|
| Solar activity prediction<br>Sunspot cycle<br>Least-squares regression<br>Solar flux | Unclassified – Unlimited<br>Robert L Holland |

| 19. SECURITY CLASSIF. (of this report) | 20. SECURITY CLASSIF. (of this page) | 21. NO. OF PAGES | 22. PRICE |
|---|---|---|---|
| Unclassified | Unclassified | 56 | NTIS |



For sale by National Technical Information Service, Springfield, Virginia 22161

## ACKNOWLEDGMENTS

The authors are indebted to many others who contributed valuable support and guidance in the development of this report and its preparation. In particular, we are grateful for the guidance and review by Dr. W. W. Vaughan, the discussions and interest of Drs. G. H. Fichtl, R. E. Smith, and Robert Turner, and the review and suggestions of Dr. Einar Tandberg-Hanssen, all of Marshall Space Flight Center's Space Sciences Laboratory, and Mr. Jesse Smith of NOAA. Also, the computer programs and data files developed by John Hickey of A.C.I. were very useful. The daily operation and programming of Chow Wei Ming of Boeing for the monthly forecast reports are also appreciated. We also are grateful to Betsey Phelps of Superior Technical Services and Annette Tingle of MSFC for preparation and editing of the manuscript.

TABLE OF CONTENTS

## LIST OF ILLUSTRATIONS

## LIST OF ILLUSTRATIONS (continued)

## LIST OF ILLUSTRATIONS (continued)

LIST OF ILLUSTRATIONS (continued)

## LIST OF ILLUSTRATIONS (continued)

## LIST OF ILLUSTRATIONS (concluded)

## LIST OF TABLES

TECHNICAL MEMORANDUM

# I. INTRODUCTION

The purpose of this report is to present the NASA-Marshall Space Flight Center solar activity long-range statistical estimation technique and the basis for the procedure used. The motivation for issuing the information monthly is the need for a current and systematic input for use in an upper atmosphere density model employed in satellite orbital lifetime estimates. The mission analysis and planning for spacecraft operations require estimates of orbital lifetimes for launches up to 15 years in the future relative to various orbital altitudes, inclinations, and eccentricities.

The upper atmosphere density model used [1] is based on the work an models developed by Jacchia [2,3] and his colleagues at the Smithsonian Astrophysical Observatory (SAO). A more recent model [4] uses essentially the same type solar activity input and gives more detailed information on number densities for the various constituents. To compute neutral density at the pertinent orbital altitudes and times, the model requires as inputs the 162-day mean and daily value of 10.7 cm solar flux ($F_{10.7}$) and the 3-hour interval geomagnetic index($A_p$) 6 to 9 hours prior to the time of the desired density calculation. The variability of the solar flux and geomagnetic activity precludes the long-term prediction of these daily and 3-hourly values with any degree of accuracy; therefore, smoothed values of these indices, estimated using a least-square linear regression procedure, are employed as inputs to the model. The model then predicts the neutral density values required in the computation of satellite orbital lifetime estimates.

This study presents the results of comparison studies conducted in the Atmospheric Sciences Division, Space Sciences Laboratory, Marshall Space Flight Center (MSFC), on various applications of statistical prediction methods for short-term (months) and long-term (years) forecasting of solar activity. This is one of many approaches to the estimation of future solar flux and geomagnetic activity prepared by those who have and are now doing research on the subject. There is no generally accepted statistical or deterministic procedure based on any known physical mechanism by the scientific community. The one reported here is an attempt to improve upon the statistical confidence of a linear regression procedure developed around 1949 by McNish and Lincoln.

The basic theory first suggested and applied by McNish and Lincoln [5] and later modified by Boykin and Richards [6] and improved by Rowe and Avaritt [7] is given in Appendix A. An excellent survey is also presented by Scissum [8] and Slutz, et al. [9].

# II. TECHNIQUE

## A Historical Background

McNish and Lincoln [5] suggested that the estimation of a future solar cycle, based on the mean approximation of all past solar cycles, could be improved by adding to the mean a correction proportional to the departure of the current values of the cycle from the mean cycle. However, this technique was not recommended for making projections longer than 1 year in the future.

Yu.I. Vitinskii [10] conducted a very extensive survey and analysis of solar activity forecasting methods. While recognizing the considerable importance of the problem and encouraging studies of active processes taking place on the Sun as a contribution toward the solution of the proolem, he well stated what is still the current situation. Vitinskii concluded: "...we have shown that the reliability of the results obtained using these methods still leaves much to be desired." However, his analysis showed that the linear regression method gives the best accuracy for future solar activity estimates up to a year in advance. For estimates several years in advance, the linear regression method becomes increasingly less accurate. The uncertainty of the linear regression method is given by the standard deviation estimates as computed by the least-square linear regression method reliability procedure. With the lack of any proven deterministic prediction scheme based on physical laws, the statistical predictions produced by this technique are used as a basis for calculating upper atmospheric density values needed for mission planning and analysis. We thereby have a best estimate and confidence bounds based on the available data record of solar activity.

Using data from two additional solar cycles, Boykin [6] modified the McNish-Lincoln technique so that the Zurich-smoothed sunspot number ($\bar{R}$) could be estimated for 10 years in advance, and at quarterly rather than yearly intervals.

Since the measured $\bar{F}_{10.7}$ data base is relatively short (1947 to date), the data base was extended back to 1749 using the following equation[1] to convert recorded smoothed ($\bar{R}$) data to smoothed solar flux ($\bar{F}_{10.7}$) data:

$$\bar{F}_{10.7} = 49.4 + 0.97\,\bar{R} + 17.6 \exp\,(-0.035\,\bar{R}) \quad . \tag{1}$$

The recorded data for $\bar{F}_{10.7}$ and $\bar{R}$ from 1947 to the present were used to derive equation (1). The linear correlation coefficient for equation (1) is 0.98. Equation (1) is used to construct smoothed solar flux $\bar{F}_{10.7}$ data for the period 1749 to 1946. After 1946, the measured values of the daily solar flux $F_{10.7}$ are used to compute the $\bar{F}_{10.7}$. This combined data base was then stored by cycle number and point number, Lagrange interpolated and inputed into the main linear regression subroutine.

All solar flux cycles used in the regression model data base prior to 1947 use the Zurich established sunspot number maxima as the starting point. After 1947, the maxima are based on the actual maxima from the smoothed solar flux values computed from the measured $F_{10.7}$ values.

The output of the solar activity long-range statistical scheme is an estimate of the 97.7, 50, and 2.3 percentile values of the $\bar{F}_{10.7}$ arranged in a monthly time sequence.

---

1. Developed in collaboration with Jack Slowey of Smithsonian Astrophysical Observatory.

Since the measured geomagnetic $A_p$ data base is relatively short (1932 to date), the data base was extended back to 1884 using equation (2) to convert geomagnetic $C_i$ data to geomagnetic $A_p$ data.

$$A_p = \text{Exp}\ (0.8267 + 4.3661\ C_i - 4.0832\ C_i^2 + 2.1795\ C_i^3 - 0.3536\ C_i^4)\ . \qquad (2)$$

The recorded data for $A_p$ and $C_i$ from 1932 to the present were used to derive equation (2). The linear correlation coefficient for equation (2) is 0.99. Cycles 13 through 16 computed $A_p$ values were then combined with actual $A_p$ values from 1932 through present. This combined data base was then smoothed and stored by cycle number and point number, Lagrange interpolated and put into the main linear regression subroutine.

The output of the solar activity long-range statistical scheme is an estimate of the 97.7, 50, and 2.3 percentile values of $\bar{A}_p$ arranged in a monthly time sequence.

## B. Lagrangian Least Squares Method

The Lagrangian least-squares prediction method outlined in the following steps was compared with the conventional application of the McNish-Lincoln method and also with various applications of the Lagrangian method to determine the methods which gave the best predictions of past cycles of solar activity.

1) Select all maximum (or minimum) points.

2) Determine all the Periods $\{P_j\}$.

3) Determine the average period $\bar{P}$.

4) Divide all cycle periods (in step 2) by $\bar{P}$ (the average period).

This will give an average time increment $\tau_j \equiv P_j/\bar{P}$ to be used for the jth cycle. Note that $\tau_j$ will be less than, equal to, or greater than 1 month.

5) Consider each cycle a block of data by selecting $m \simeq \bar{P}$ sunspot (or flux) points in each cycle. This will require some interpolation to obtain each sunspot (or flux) corresponding to all m points per cycle, since points are not being selected at the 1-month increment.

6) When all the cycles have been blocked in this manner, the McNish-Lincoln method can be applied to produce a prediction of the mean and $\pm 1\sigma$, $2\sigma$, and $3\sigma$ values of $\bar{F}_{10.7}$ for the next cycle, assuming that the distribution of values is Gaussian.

7) The predicted cycle time increment is approximated by averaging all the past cycle time increments. It just so happens that this time increment will be exactly equal to 1.

Proof:

$$\tau_{N+1} = \frac{1}{\bar{N}} \sum_{j=1}^{N} \tau_j = \frac{1}{\bar{N}} \sum_{j=1}^{N} \frac{P_j}{\bar{P}} = \frac{1}{N\bar{P}} \sum_{j=1}^{N} P_j = \frac{\frac{1}{\bar{N}} \sum_{j=1}^{N} P_j}{\frac{1}{\bar{N}} \sum_{j=1}^{N} P_j} = 1 \qquad (3)$$

N is the number of past cycles.

$P_j$ is the period of the jth cycles.

8) The interpolation mentioned in step 5 is accomplished by applying a conventional Lagrangian method from the MSFC math-pack computer program library [11].

9) The predicted cycle period will be the average period $\bar{P}$ plus or minus its $2\sigma$ value; i.e., $\bar{P} \pm 2\sigma_p$.

10) The $2\sigma_p$ error band on the time axis combined with the $2\sigma_R$ error band on the sunspot (or flux) values will give the "error space" on the two-dimensional plot of R versus t.

## III. SINGLE CYCLE PREDICTION

The preceding procedure was applied, with the number of points per cycle (m) being 132. This number was selected because it is the closest integer to the average period in months. A single cycle was then predicted using the previous 16 cycles (from 1749) in order to predict cycle 17 for comparison with the actual observations. This process was then repeated in order to predict cycles 17, 18, 19, and 20 by the conventional McNish-Lincoln method and the Lagrangian least-squares approach.

This particular statistic gives a relatively simple and easily applied criterion for judging and comparing goodness of fit of various models (or expected values) of observed data. For large degrees of freedom, the standard chi-square distribution approaches the normal distribution. It also gives a standard, acceptable and fair way of determining those models (or portions of the models) which fall within the conventional 95 percentile level of confidence.

Table 1 gives a summary of the results of the preceding method. The entries are the calculated $\chi^2$ (0.05) by Pearson's chi-square statistics [12]; i.e.,

$$\chi^2 = \sum_{j=1}^{m} \frac{(O_i - E_i)^2}{E_i} , \qquad (4)$$

where $O_i$ is observed and $E_i$ is the expected (predicted) value.

TABLE 1. SINGLE CYCLE $\chi^2(0.05)$

| Method | 17 | 18 | 19 | 20 |
|---|---|---|---|---|
| McNish-Lincoln | | | | |
| 1 Coefficient | 721 | 1687 | 268 | 400 |
| 4 Coefficient | 1404 | 6128 | 236 | 304 |
| Lagrangian | | | | |
| 1 Coefficient | 277 | 1193 | 155 | 177 |
| 4 Coefficient | 753 | 513 | 1221 | 183 |

Note: These are to be compared with the $\chi^2(0.05, 127)$ and $\chi^2(0.05, 130)$ values from the standard chi-square tables, which are 154 and 158.

Table 1 shows that the Lagrangian least squares approach produces a significantly better prediction of the next solar cycle than the McNish-Lincoln technique with the exception of cycle 18.

## IV. EXTENDED AND DOUBLE CYCLE PREDICTION

This section presents descriptions of the six methods for extended predictions which were compared, again using Pearson's chi-square statistics [see Eq. (4)].

The double-cycle McNish-Lincoln technique applied the standard regression program to the data blocked in 262 points per block, which is approximately 22 years or two average cycle periods. The 262 points started at the maximum and ended 262 months later.

The double-cycle Lagrangian technique blocked the data into double cycles of 262 points which started at the maximum and ended at a maximum two cycles later. This necessitates interpolation because the time increment between points varies from block to block.

The technique of Langrangian prediction connected to the mean at the minimum blocks the data into single cycles of 132 points per cycle. The 132 points start at the maximum and end at the next maximum. A future cycle is predicted to the next minimum and then patched (connected with a cubic at the nearest inflection point 2 years before the maximum) to the mean cycle for the remaining part of the extended prediction (see Appendix B for cubic connection).

The technique of Lagrangian prediction connected to the mean at the maximum technique is similar to the preceding technique except that the prediction is over a full future cycle to the next maximum and then connected to the mean cycle for the remaining part of the extended prediction.

The iterated Lagrangian technique predicts over a full cycle, treats the predicted data as actual data, and then predicts over another future cycle.

The Lagrangian derivative technique includes the influence of the rate of change of the deviations from the mean cycle in the regression scheme. The regression model has this term added in the same way as the deviations are included,

$$R_{m+k,j} = \bar{R}_{m+k,j} + \sum_{q=1}^{m} (C_{q,k}\, \Delta R_{q,j} + d_{q,k}\, \Delta \dot{R}_{q,j}) \,. \tag{5}$$

If the derivative influence is zero, the $d_{q,k}$ coefficients will be zero or the first m $\Delta \dot{R}$'s will be zero.

Each of the preceding methods was applied to predict cycles 15 through 20 by using all the previous cycles to the one being predicted. Since actual or observed data and expected or predicted data were then available, Pearson's [12] chi-square could be calculated at each point of the cycle (beyond, say, 10 or 20 for a significant number of degrees of freedom). The results of applying the methods above are shown in Figures 1 through 40.

The even figure plots (2, 4, 6, .... 40) give the predicted solar flux (.), the actual smoothed values (*), the plus 2$\sigma$ error (+), and the minus 2$\sigma$ (-) error bands. The plus and minus 2$\sigma$ error was calculated using the predicted (expected) values of the current cycle or cycles minus the actual 13-month smoothed Lagrangian values at corresponding points of all previous cycles for the deviations.

$$\sigma_i = \left( \frac{\sum_{j=1}^{N} (E_{ij} - O_{ij})^2}{N-1} \right)^{\frac{1}{2}} \,, \tag{6}$$

where i refers to the Lagrangian point in the cycle and N is the number of known past cycles.

The odd figure plots (1, 3, 5 ..., 39) give the $\chi^2$ versus point number (i) in the cycle together with the standard $\chi^2$ (0.05) at the 0.05 level of significance versus points (i) in the cycle. Table 2 presents the overall chi-square comparisons for the full extended predictions. It can be seen again that the Lagrangian technique gave a better chi-square than the McNish-Lincoln, but it still was not within the 95 percentile level of confidence given in the right column, except for cycles 15 and 16. It may also be noted that not one of the methods tried did well on cycles 18 and 19. This suggests that the long period effect (7 or 8 cycles) referred to in the literature and in Section VI cannot be predicted by any of the methods tried thus far. From the plots one can determine how well the prediction method is doing as it progresses through the cycle and beyond. The plots also show when the method is within the 0.05 level of significance.

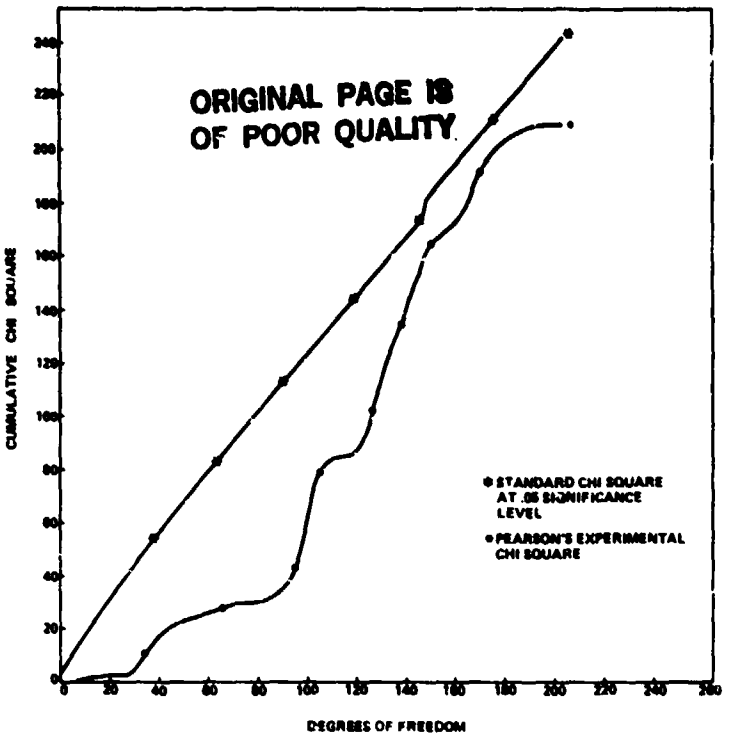


Figure 1. Chi square versus point number (nominally months), 13-month Lagrangian-smoothed flux (extended by median cycle from min.), 1 coefficient linear model using 1 through 14 predicting cycles 15, and 16 from point 1.

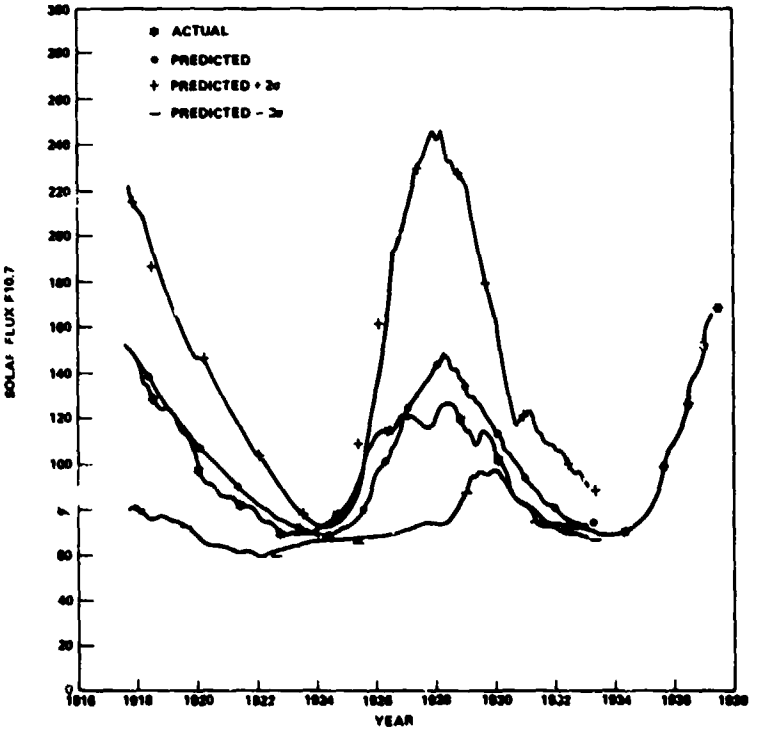


Figure 2. Predicted and actual flux versus time, 13-month Lagrangian-smoothed flux (extended by median cycle from min.), 1 coefficient linear model using cycles 1 through 14 predicting cycles, 15 and 16 from point 1.

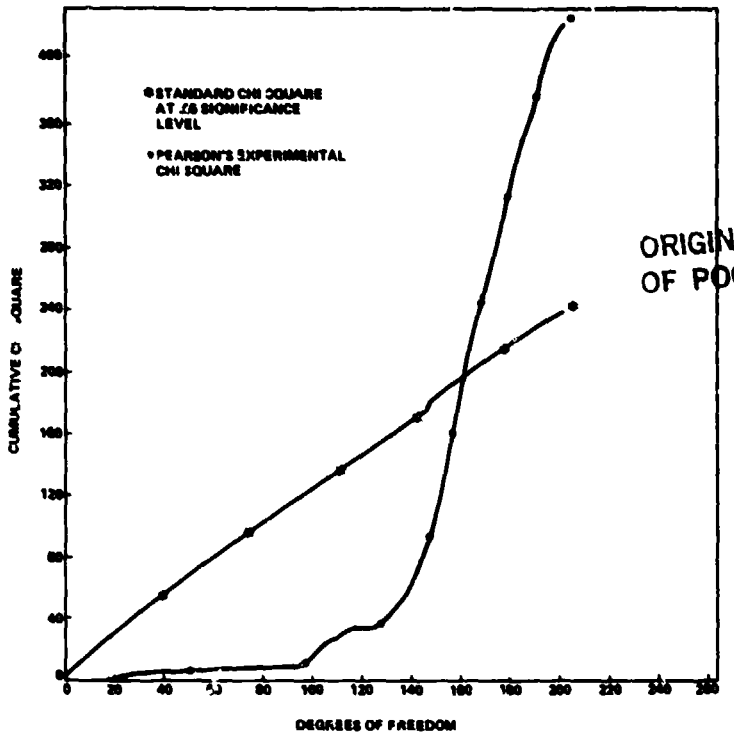




Figure 3. Chi square versus point number (nominally months) 13-month Lagrangian-smoothed flux (extended by median cycle from min.) 1 coefficient linear model using cycles 1 through 15 predicting cycles 16 and 17 from point 1.

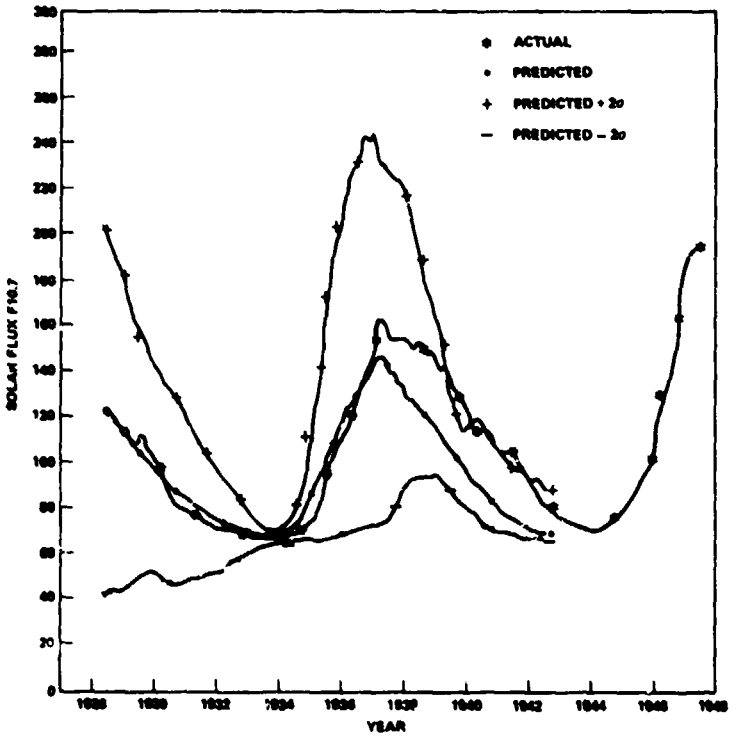


Figure 4. Predicted and actual flux versus time 13-month Lagrangian-smoothed flux (extended by median cycle from min.) 1 coefficient linear model using cycles 1 through 15 predicting cycles 16 and 17 from point 1.

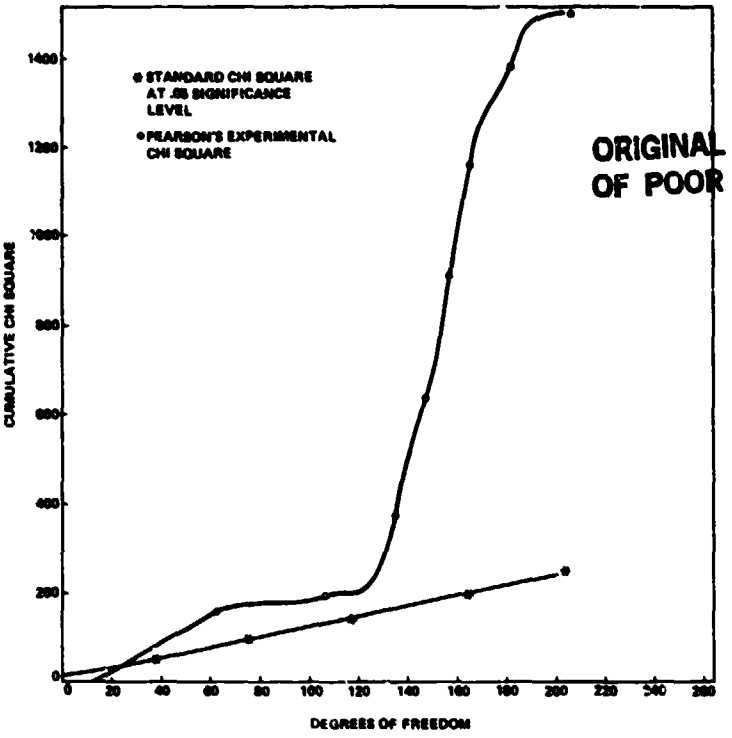




Figure 5. Chi square versus point number (nominally months) 13-month Lagrangian-smoothed flux (extended by median cycle from min.) 1 coefficient linear model using cycles 1 through 16 predicting cycles 17 and 18 from point 1.

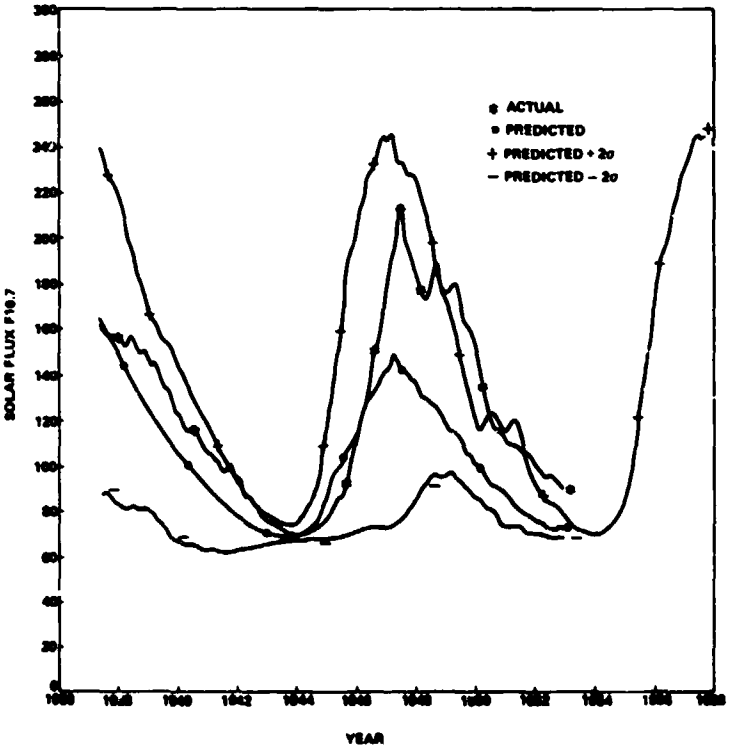


Figure 6. Predicted and actual flux versus time 13-month Lagrangian-smoothed flux (extended by median cycle from min.) 1 coefficient linear model using cycles 1 through 16 predicting 17 and 18 from point 1.

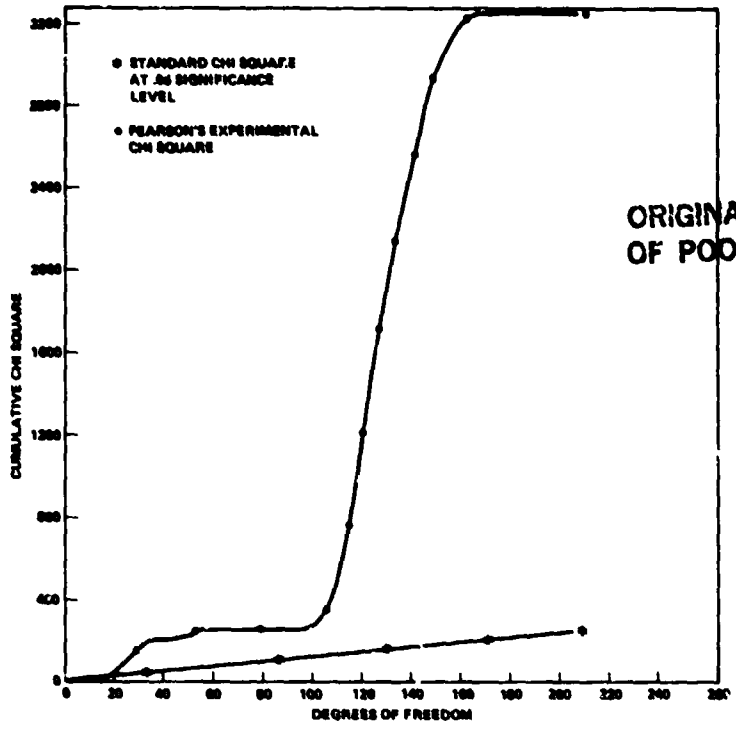




Figure 7. Chi square versus point number (nominally months), 13-month Lagrangian-smoothed flux (extended by median cycle from min.) 1 coefficient linear model using cycles 1 through 17 predicting cycles 18 and 19 from point 1.

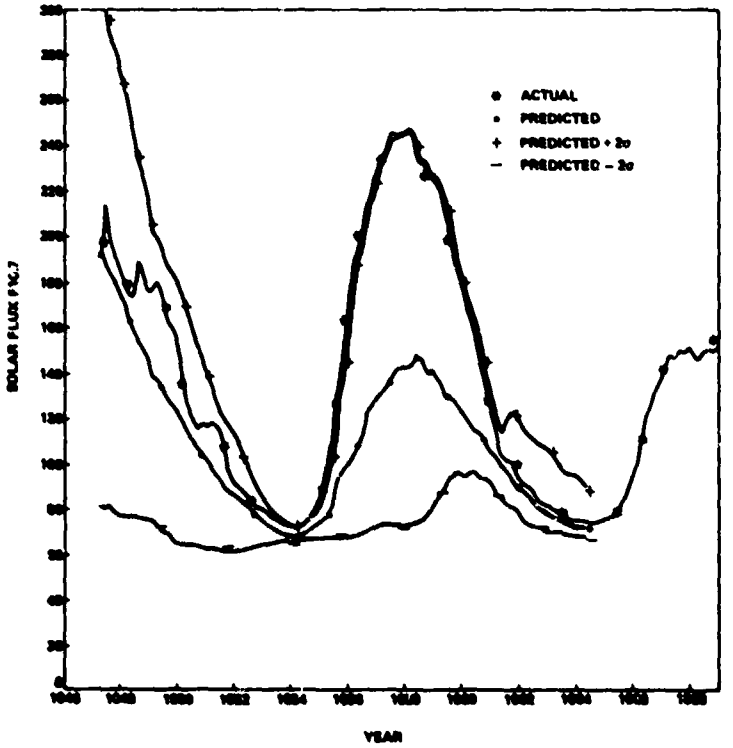


Figure 8. Predicted and actual flux versus time 13-month Lagrangian-smoothed flux (extended by median cycle from min.) 1 coefficient linear model using cycles 1 through 17 predicting cycles 18 and 19 from point 1.

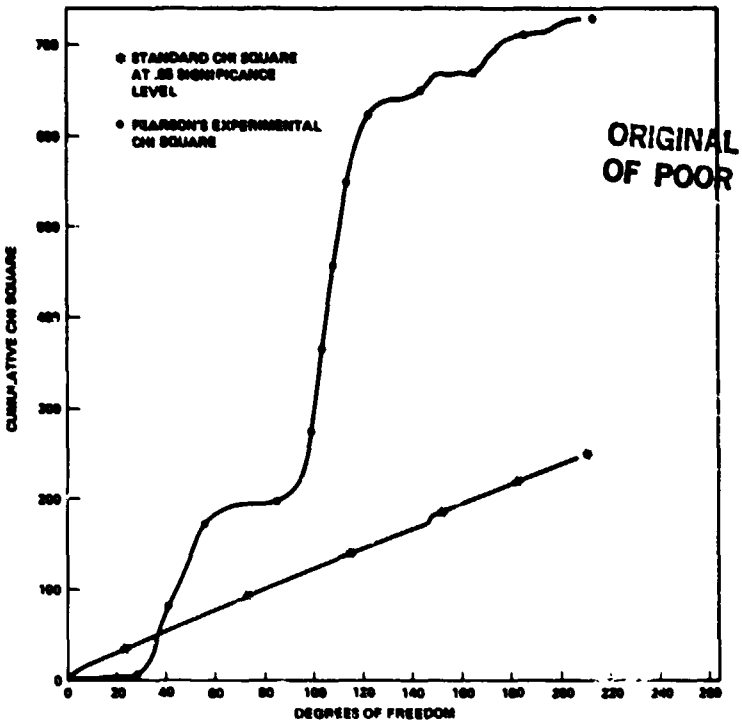




Figure 9. Chi square versus point number (nominally months) 13-month Lagrangian-smoothed flux (extended by median cycle from min.) 1 coefficient linear model using cycles 1 through 18 predicting cycles 19 and 20 from point 1.

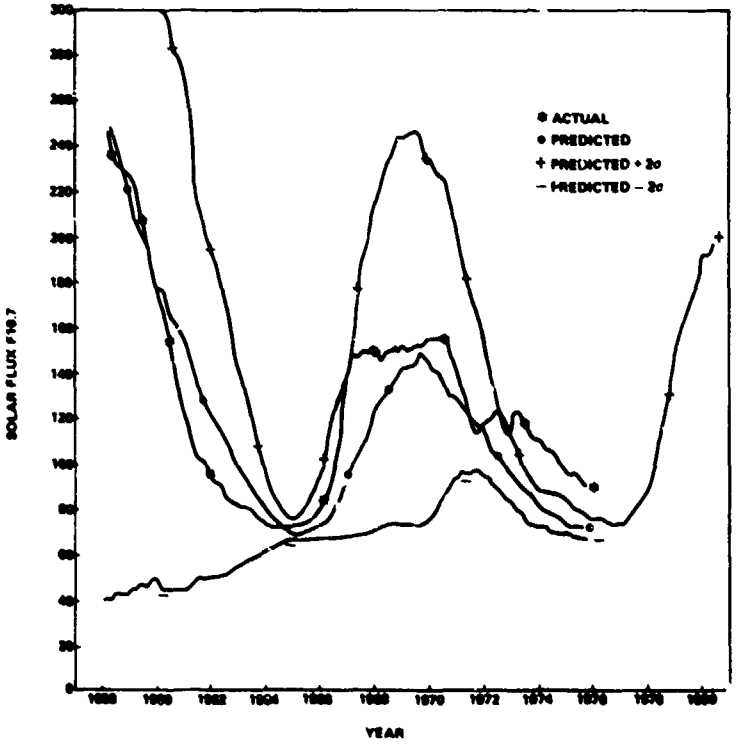


Figure 10. Predicted and actual flux versus time 13-month Lagrangian-smoothed flux (extended by median cycle from min.) 1 coefficient linear model using cycles 1 through 18 predicting cycles 19 and 20 from point 1.

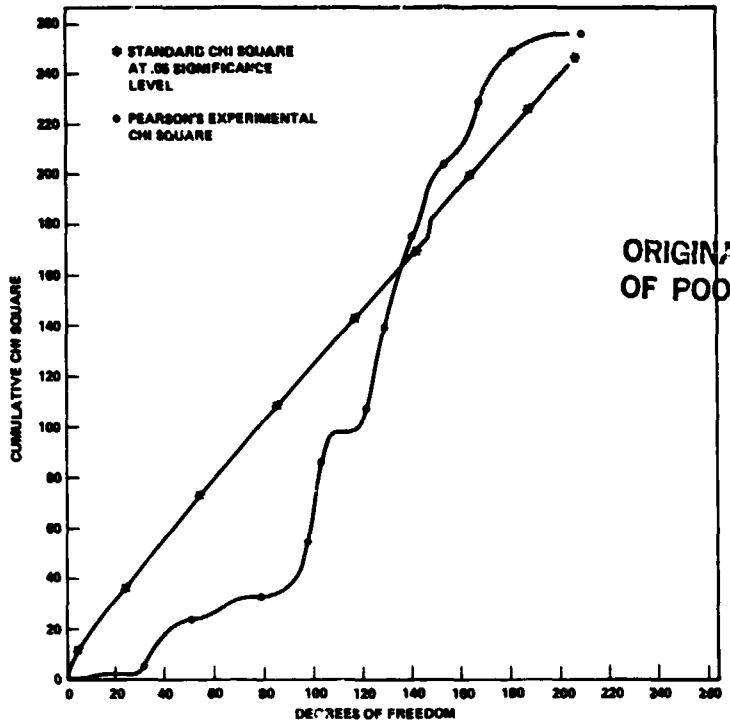




Figure 11. Chi square versus point number (nominally months) 13-month Lagrangian-smoothed flux (extended by median cycle from max.) 1 coefficient linear model using cycles 1 through 14 predicting cycles 15 and 16 from point 1.

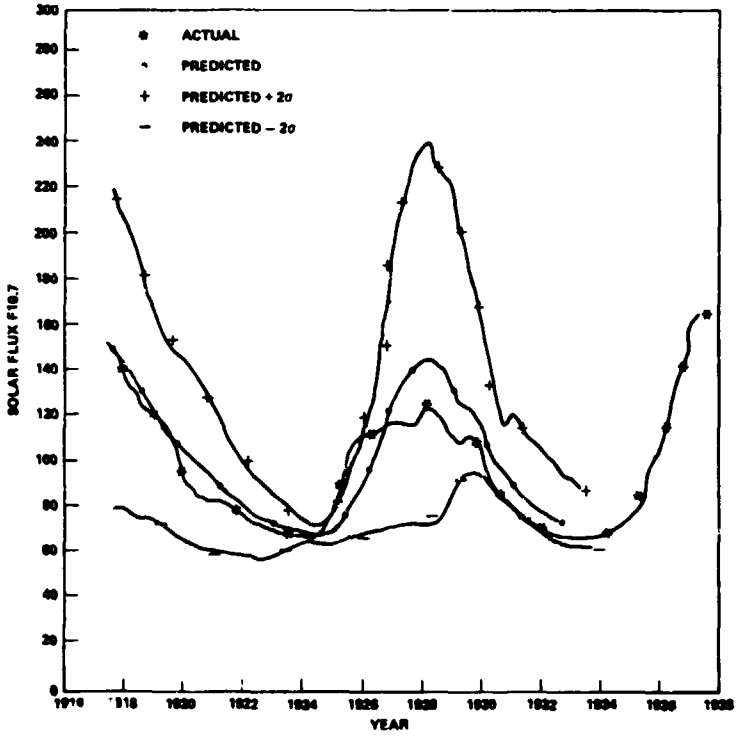


Figure 12. Predicted and actual flux versus time 13-month Lagrangian-smoothed flux (extended by median cycle from max.) 1 coefficient linear model using cycles 1 through 14 predicting cycles 15 and 16 from point 1.

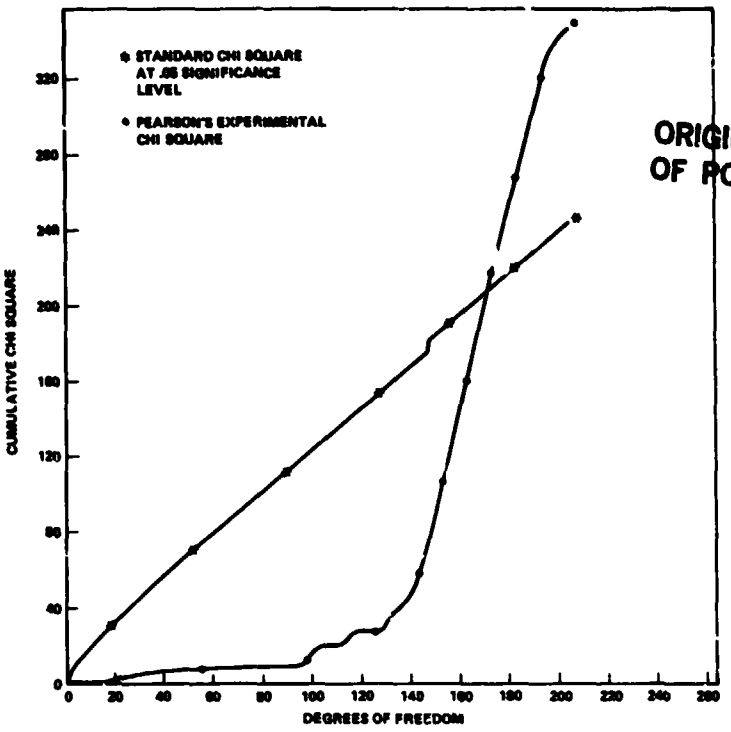




Figure 13. Chi square versus point number (nominally months) 13-month Lagrangian-smoothed flux (extended by median cycle from max.) 1 coefficient linear model using cycles 1 through 15 predicting cycles 16 and 17 from point 1.

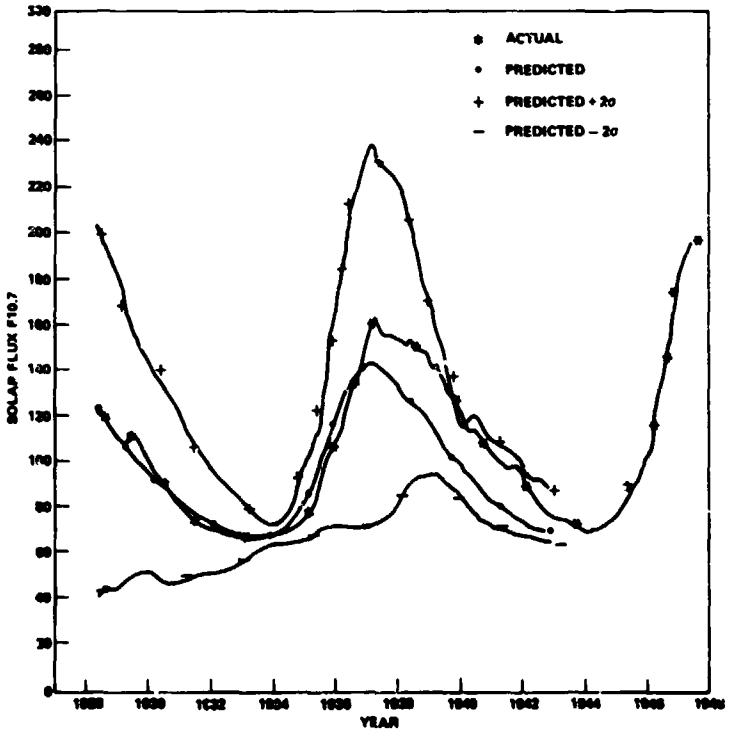


Figure 14. Predicted and actual flux versus time 13-month Lagrangian-smoothed flux (extended by median cycle from max.) 1 coefficient linear model using cycles 1 through 15 predicting cycles 16 and 17 from point 1.

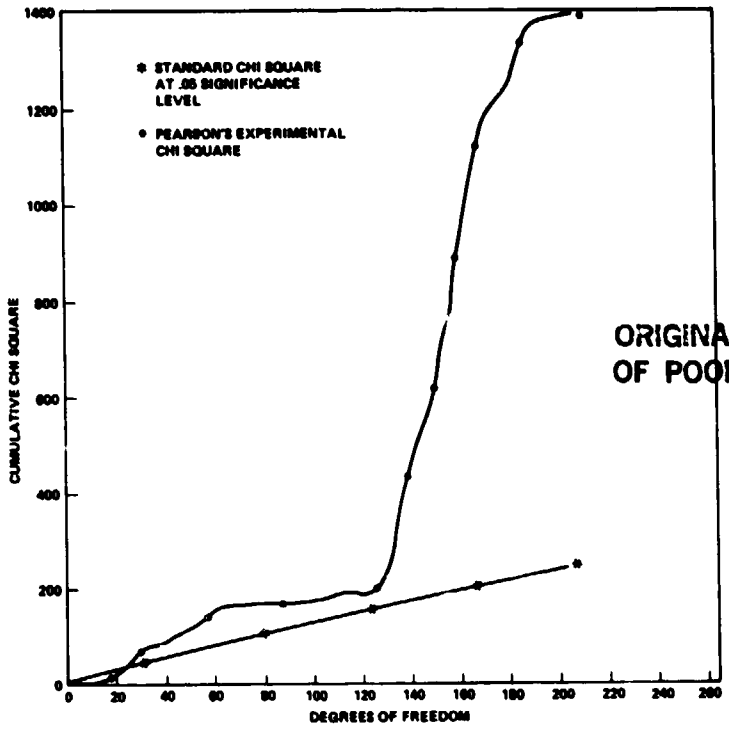


Figure 15. Chi square versus point number (nominally months) 13-month Lagrangian-smoothed flux (extended by median cycle from max.) 1 coefficient linear model using cycles 1 through 16 predicting cycles 17 and 18 from point 1.

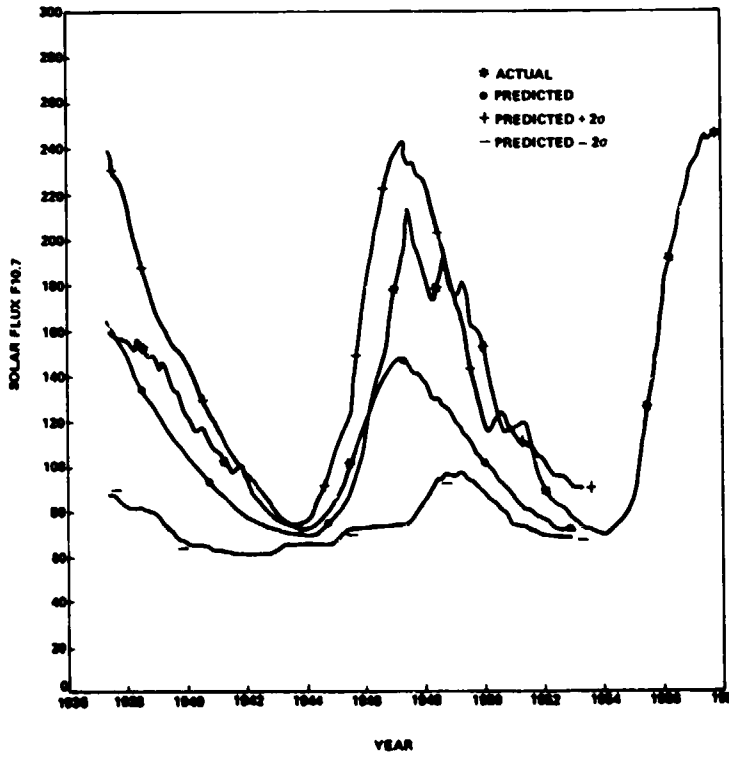


Figure 16. Predicted and actual flux versus time 13-month Lagrangian-smoothed flux (extended by median cycle from max.) 1 coefficient linear model using cycles 1 through 16 predicting cycles 17 and 18 from point 1.

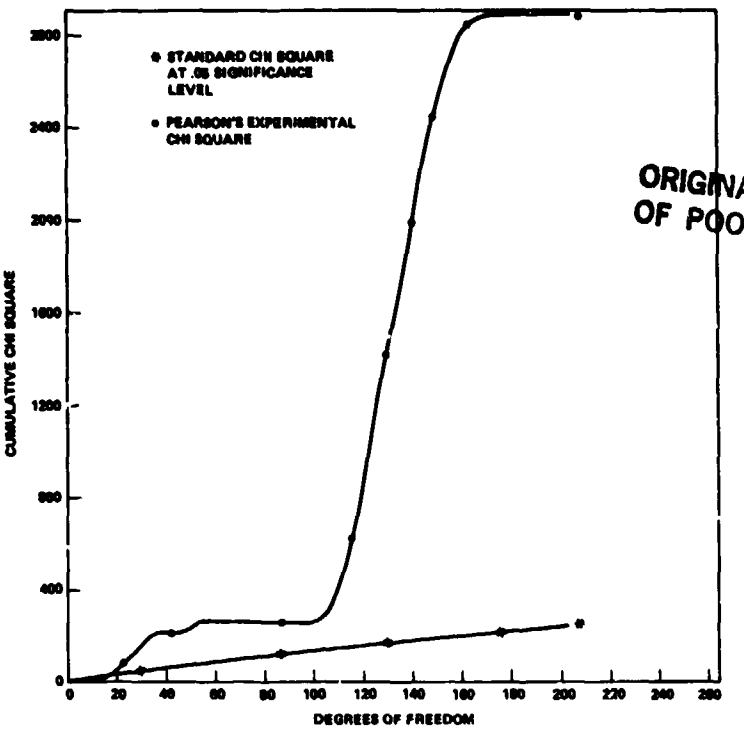




Figure 17. Chi square versus point number (nominally months) 13-month Lagrangian-smoothed flux (extended by median cycle from max.) 1 coefficient linear model using cycles 1 through 17 predicting cycles 18 and 19 from point 1.

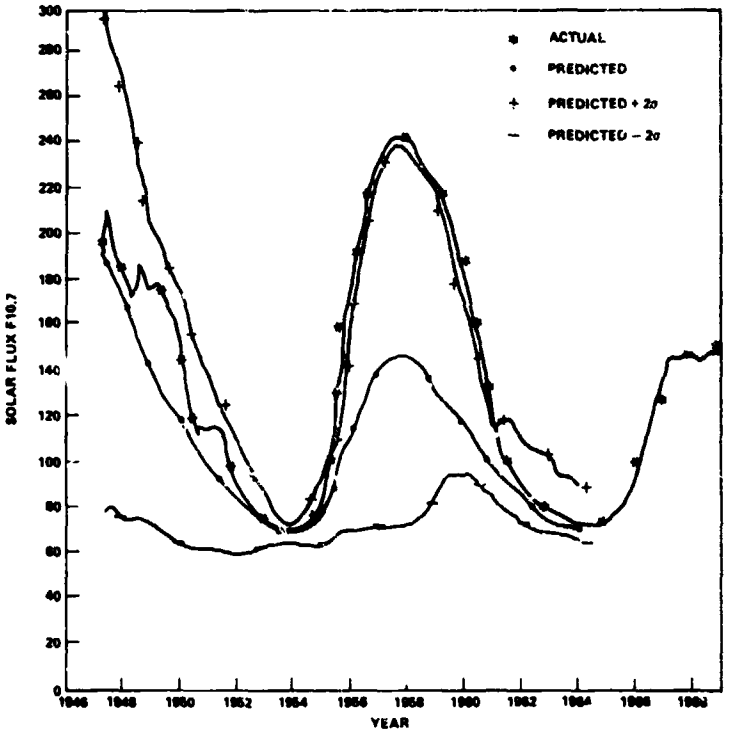


Figure 18. Predicted and actual flux versus time 13-month Lagrangian-smoothed flux (extended by median cycle from max.) 1 coefficient linear model using cycles 1 through 17 predicting cycles 18 and 19 from point 1.

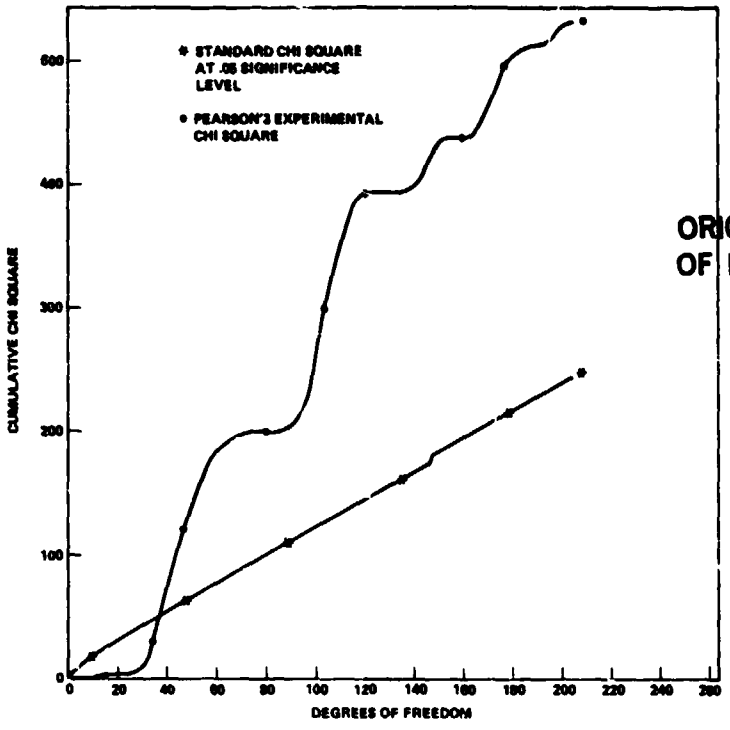




Figure 19. Chi square versus point number 13-month Lagrangian-smoothed flux (extended by median cycle from max.) 1 coefficient linear model using cycles 1 through 18 predicting cycles 19 and 20 from point 1.

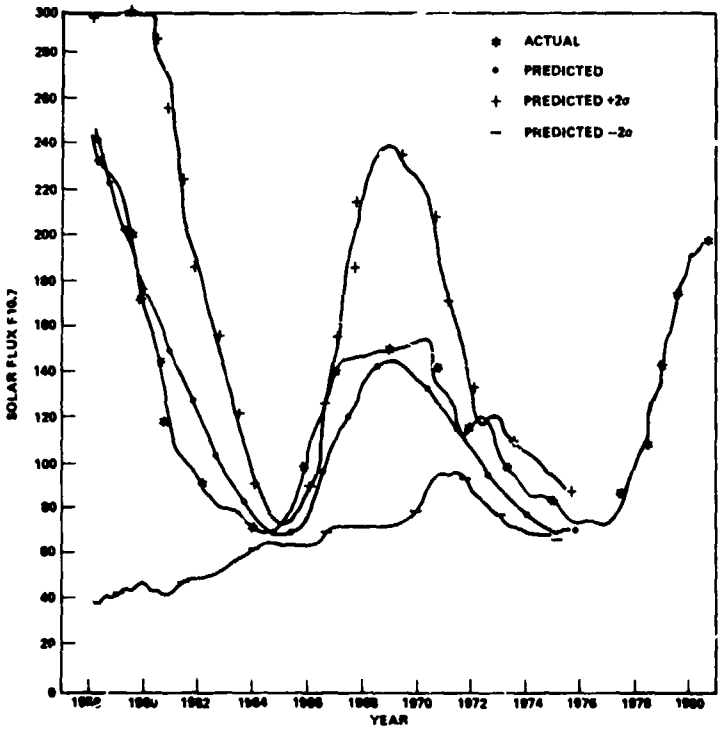


Figure 20. Predicted and actual flux versus time 13-month Lagrangian-smoothed flux (extended by median cycle from max.) 1 coefficient linear model using cycles 1 through 18 predicting cycles 19 and 20 from point 1.

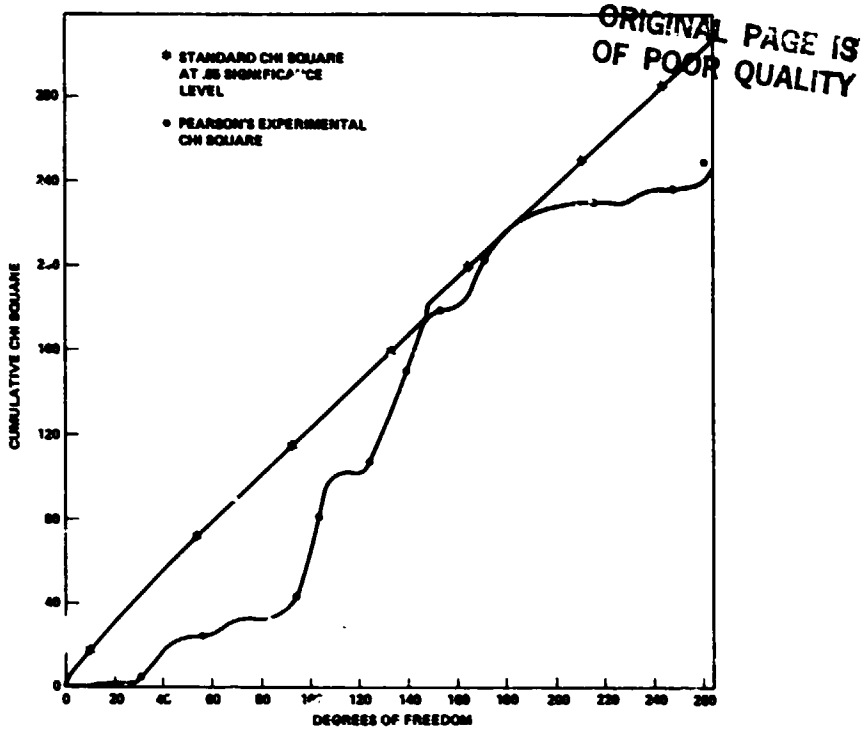


Figure 21. Chi square versus point number (nominally months) 13-month Lagrangian-smoothed flux (extended by iterated McNish-Lincoln) 1 coefficient linear model using cycles 1 through 14 predicting cycles 15 and 16 from point 1.

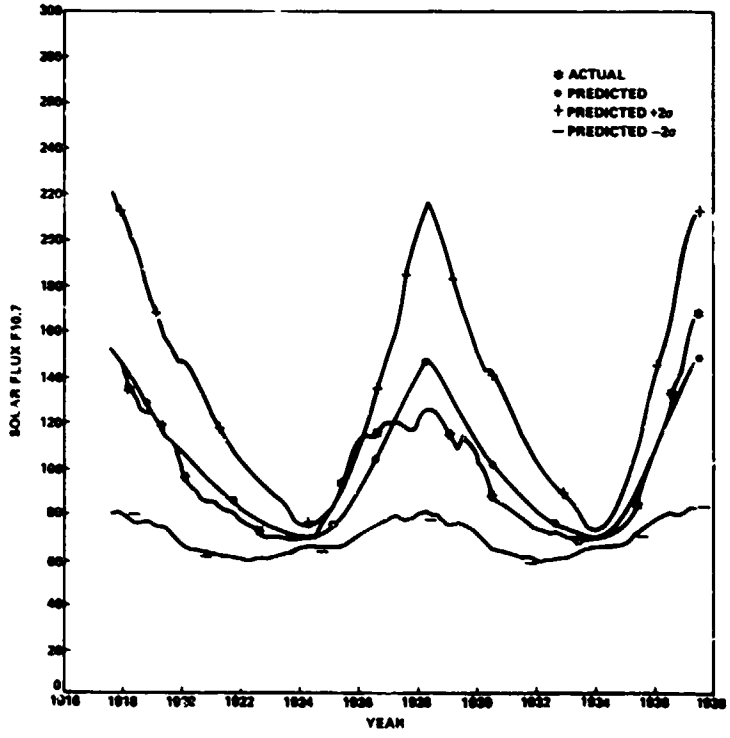


Figure 22. Predicted and actual flux versus time 13-month Lagrangian-smoothed flux (extended by iterated McNish-Lincoln) 1 coefficient linear model using cycles 1 through 14 predicting cycles 15 and 16 from point 1.

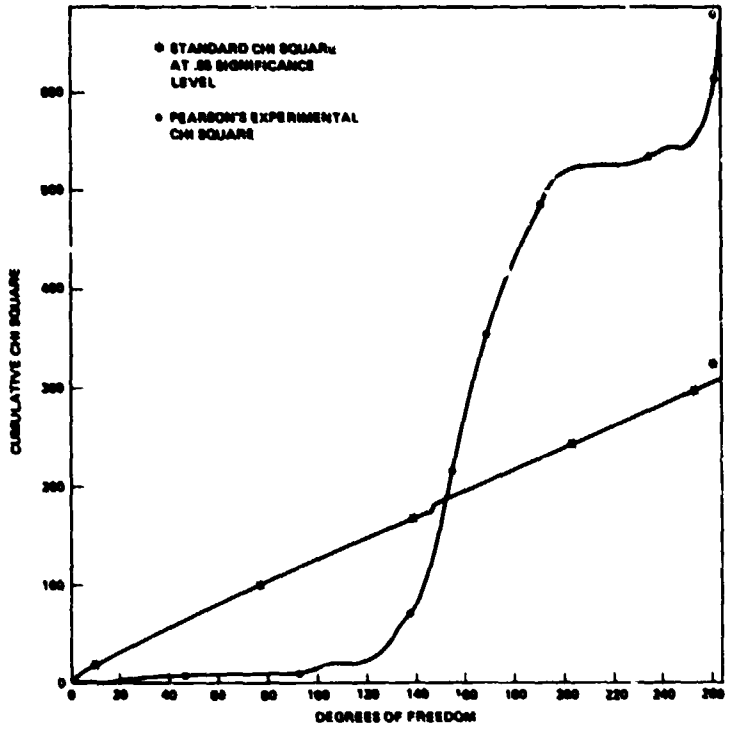


Figure 23. Chi square versus point number (nominally months) 13-month Lagrangian-smoothed flux (extended by iterated McNish-Lincoln) 1 coefficient linear model using cycles 1 through 15 predicting cycles 16 and 17 from point 1.

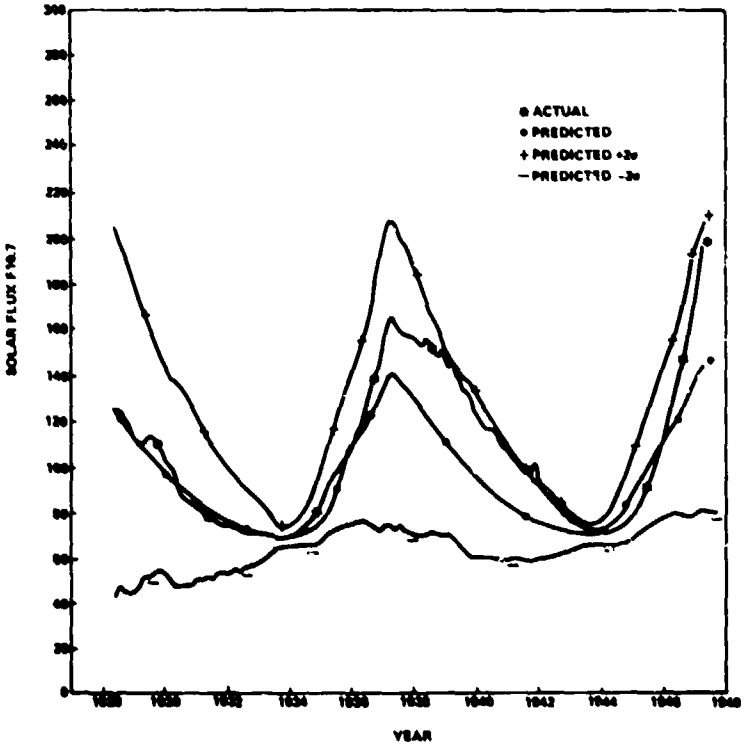


Figure 24. Predicted and actual flux versus time 13-month Lagrangian-smoothed flux (extended by iterated McNish-Lincoln) 1 coefficient linear model using cycles 1 through 15 predicting cycles 16 and 17 from point 1.

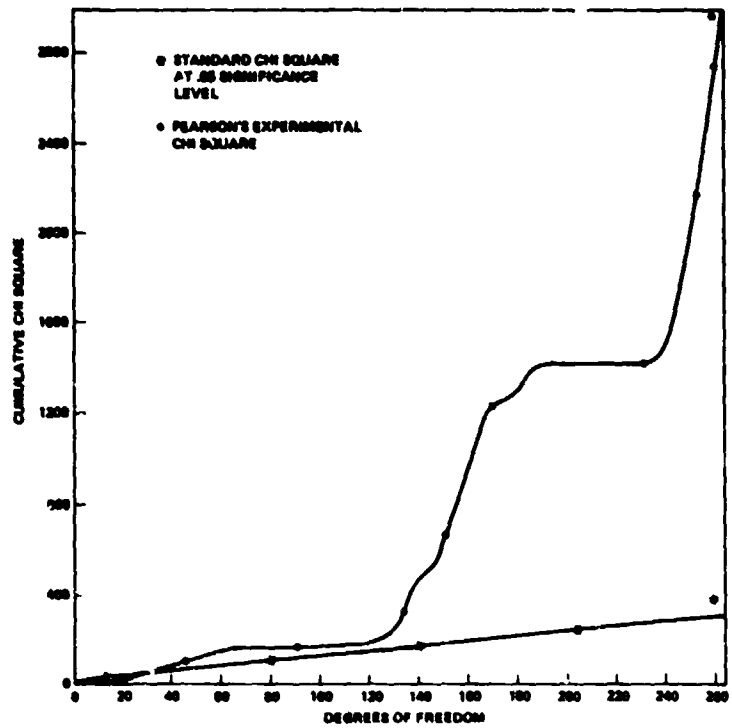


Figure 25. Chi square versus point number (nominally months) 13-month Lagrangian-smoothed flux (extended by iterated McNish-Lincoln) 1 coefficient linear model using cycles 1 through 16 predicting cycles 17 and 18 from point 1.

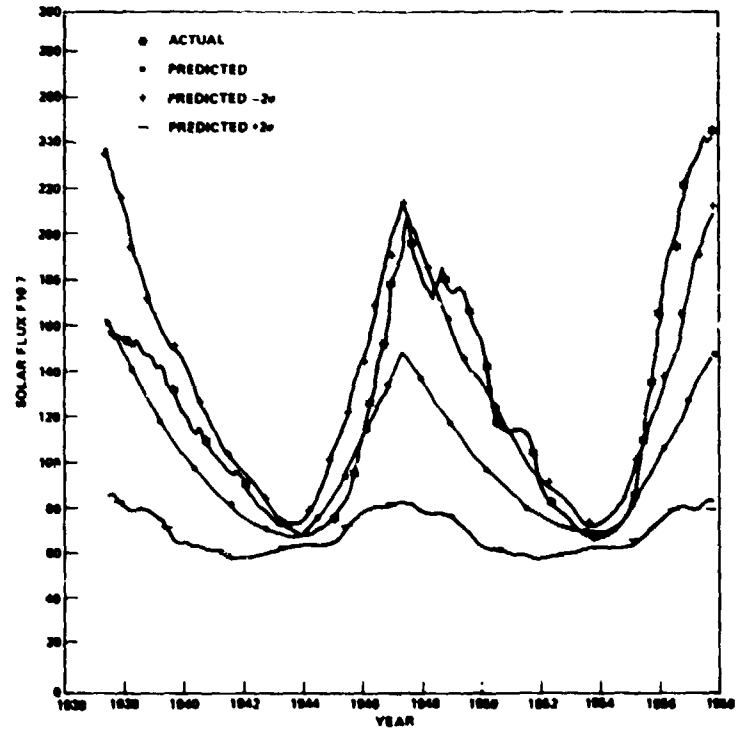


Figure 26. Predicted and actual flux versus time 13-month Lagrangian-smoothed flux (extended by iterated McNish-Lincoln) 1 coefficient linear model using cycles 1 through 16 predicting cycles 17 and 18 from point 1.

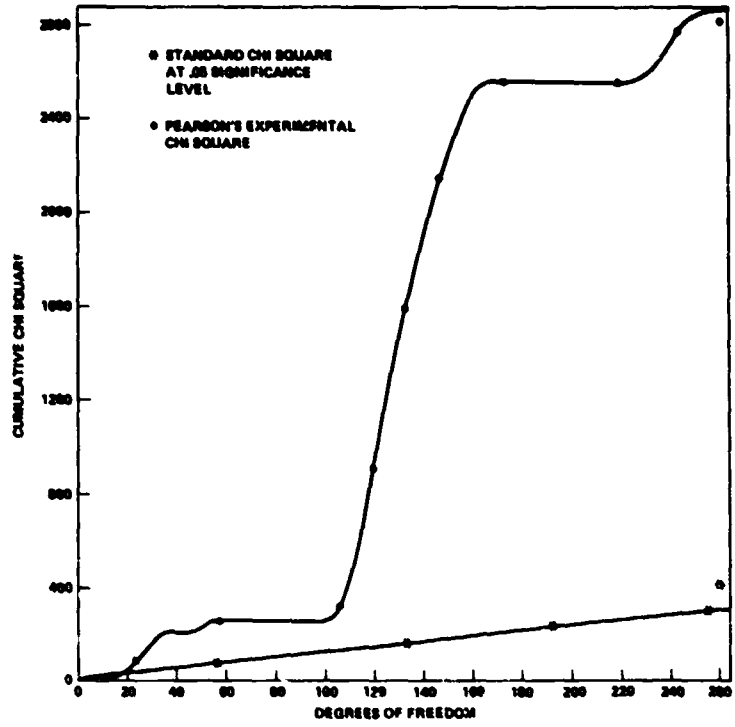


Figure 27. Chi square versus point number (nominally months) 13-month Lagrangian-smoothed flux (extended by iterated McNish-Lincoln) 1 coefficient linear model using cycles 1 through 17 predicting cycles 18 and 19 from point 1.

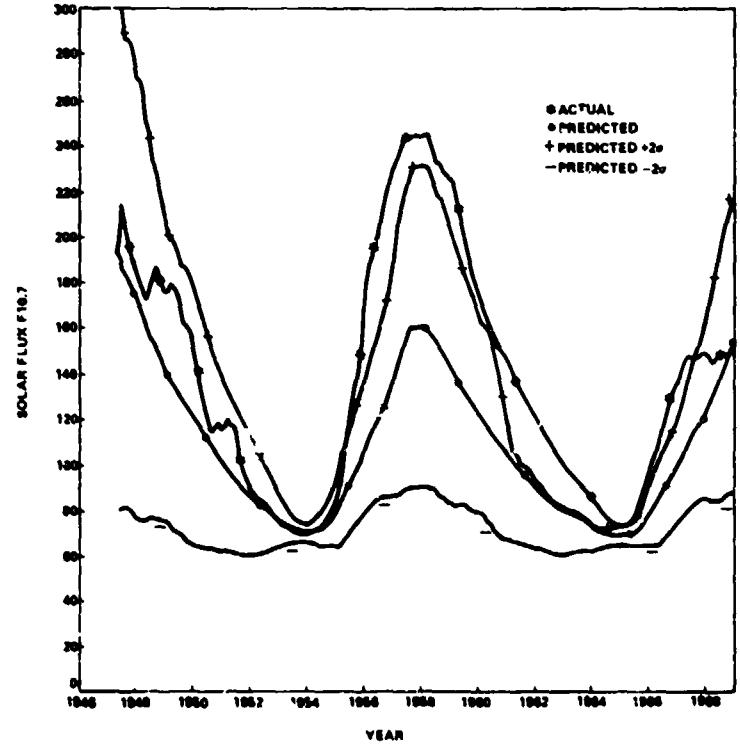


Figure 28. Predicted and actual flux versus time 13 month Lagrangian-smoothed flux (extended by iterated McNish-Lincoln) 1 coefficient linear model using cycles 1 through 17 predicting cycles 18 and 19 from point 1.

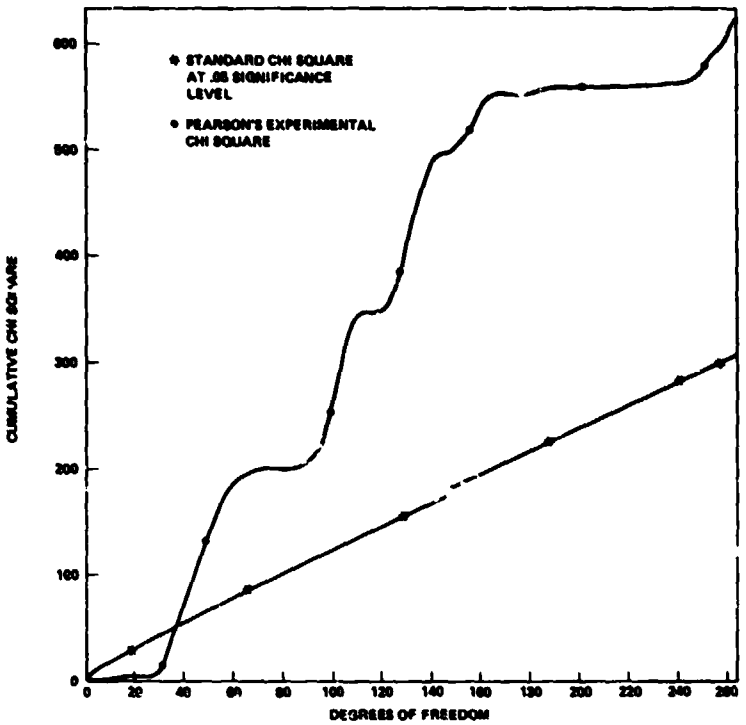


Figure 29. Chi square versus point number (nominally months) 13-month Lagrangian-smoothed flux (extended by iterated McNish-Lincoln) 1 coefficient linear model using cycles 1 through 18 predicting cycles 19 and 20 from point 1.

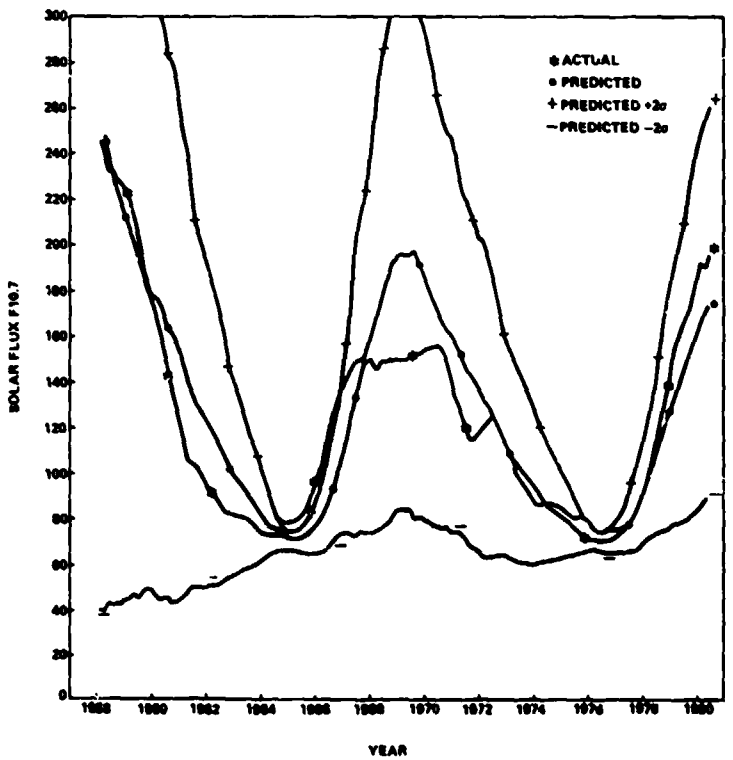


Figure 30. Predicted and actual flux versus time 13-month Lagrangian-smoothed flux (extended by iterated McNish-Lincoln) 1 coefficient linear model using cycles 1 through 18 predicting cycles 19 and 20 from point 1.

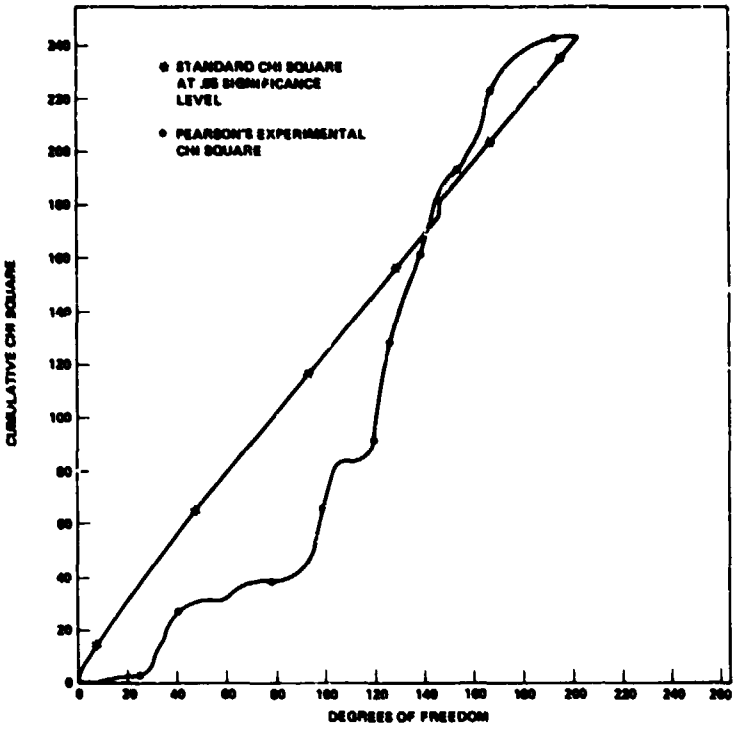


Figure 31. Chi square versus poi. t number (nominally months) 13-month ! Lagrangian-smoothed flux (extended by derivative and connected to median cycle from max.) 1 coefficient linear model using cycles 1 through 14 predicting cycles 15 and 16 from point 2.

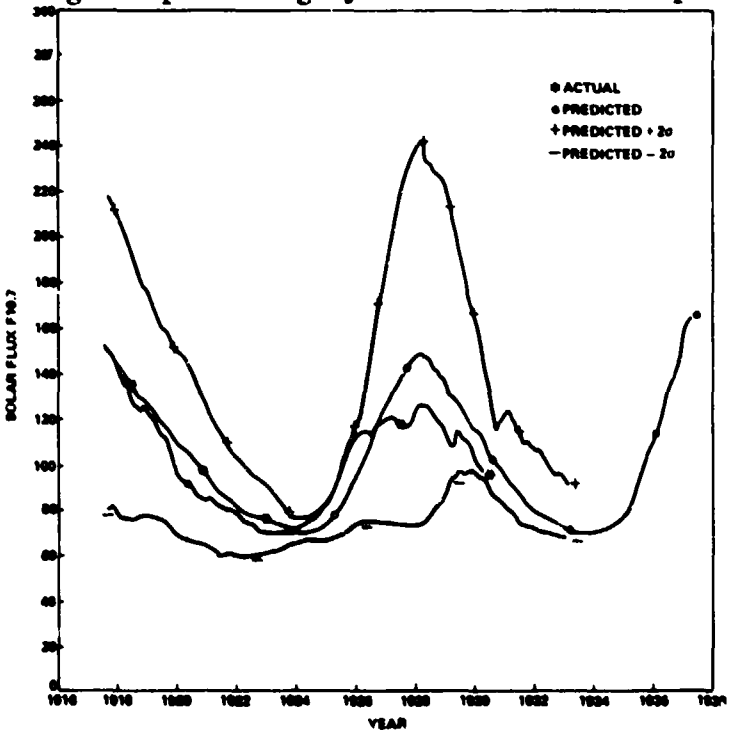


Figure 32. Predicted and actual flux versus time 13-month Lagrangian-smoothed flux (extended by derivative and connected to median cycle from max.) 1 coefficient linear model using cycles 1 through 14 predicting cycles 15 and 16 from point 2.

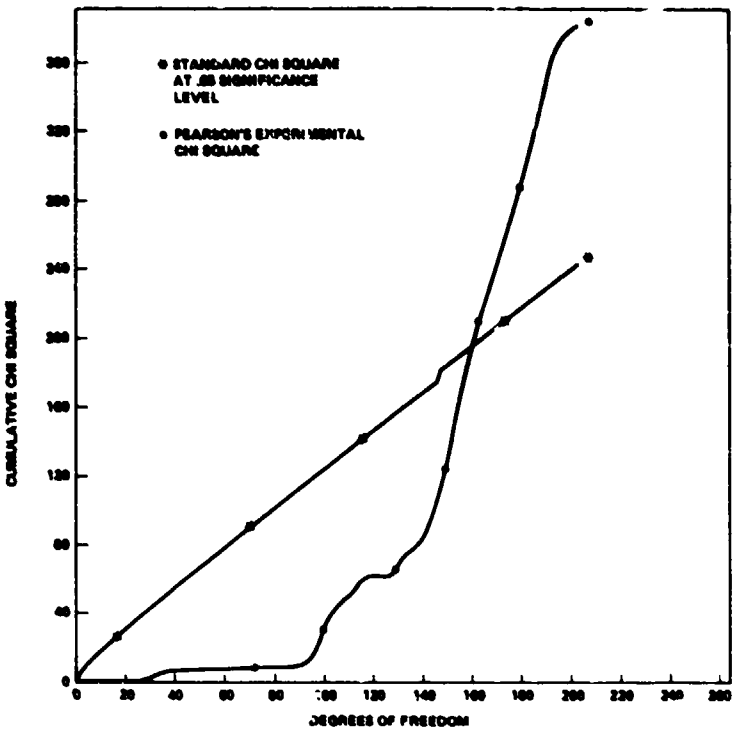


Figure 33. Chi square versus point number (nominally months) 13-month Lagrangian-smoothed flux (extended by derivative and connected to median cycle from max.) 1 coefficient linear model using cycles 1 through 15 predicting cycles 16 and 17 from point 2.

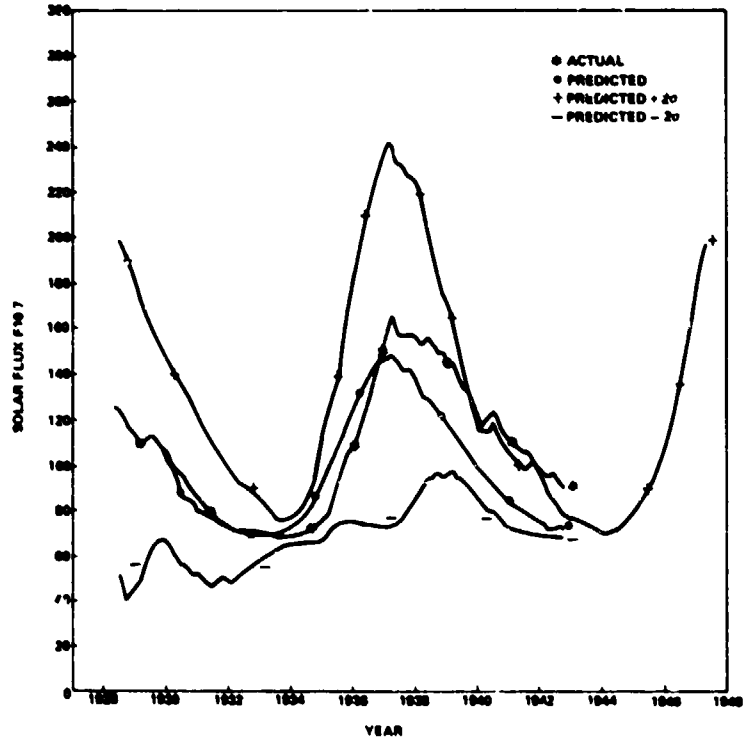


Figure 34. Predicted and actual flux versus time 13-month Lagrangian-smoothed flux (extended by derivative and connected to median cycle from max.) 1 coefficient linear model using cycles 1 through 15 predicting cycles 16 and 17 from point 2.

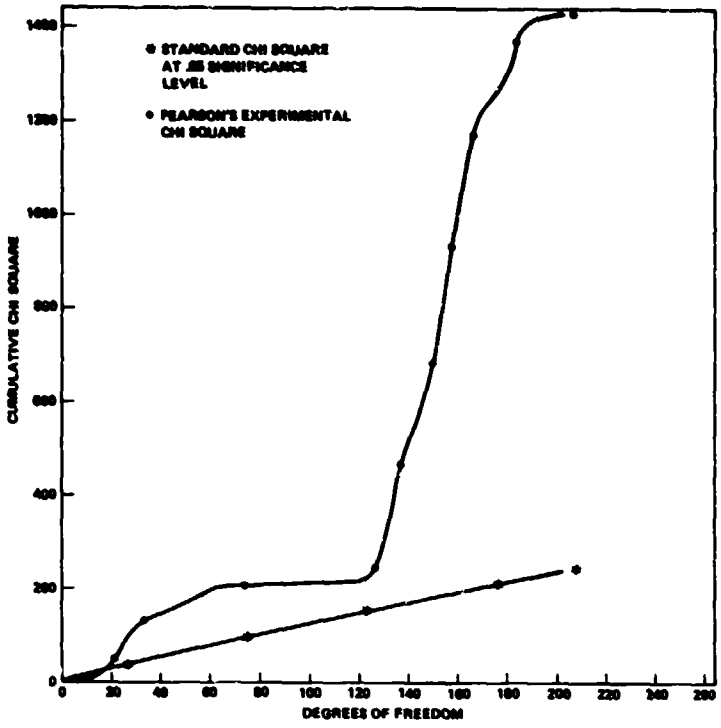


Figure 35. Chi square versus point number (nominally months) 13-month Lagrangian-smoothed flux (extended by derivative and connected to median cycle from max.) 1 coefficient linear model using cycles 1 through 16 predicting cycles 17 and 18 from point 2.

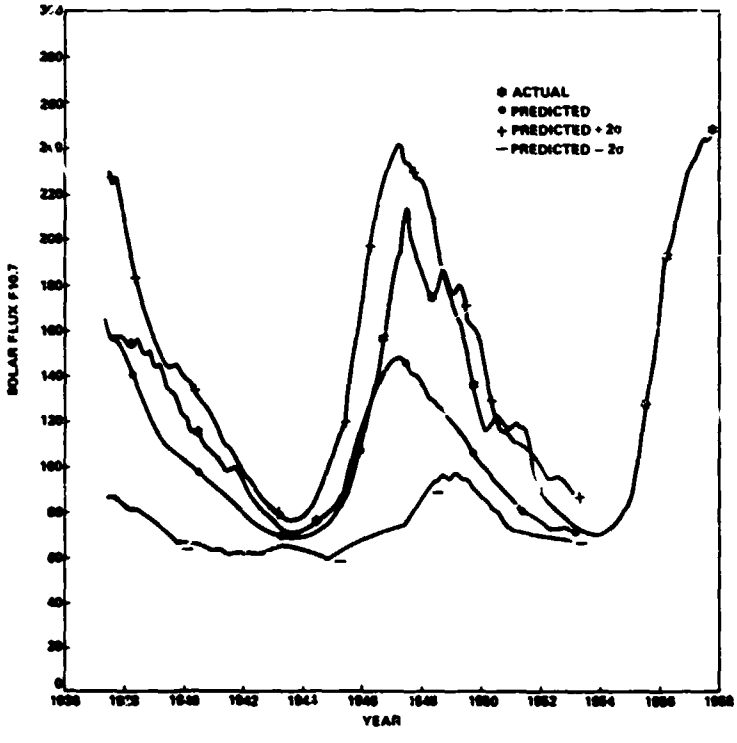


Figure 36. Predicted and actual flux versus time 13-month Lagrangian-smoothed flux (extended by derivative and connected to median cycle from max.) 1 coefficient linear model using cycles 1 through 16 predicting cycles 17 and 18 from point 2.

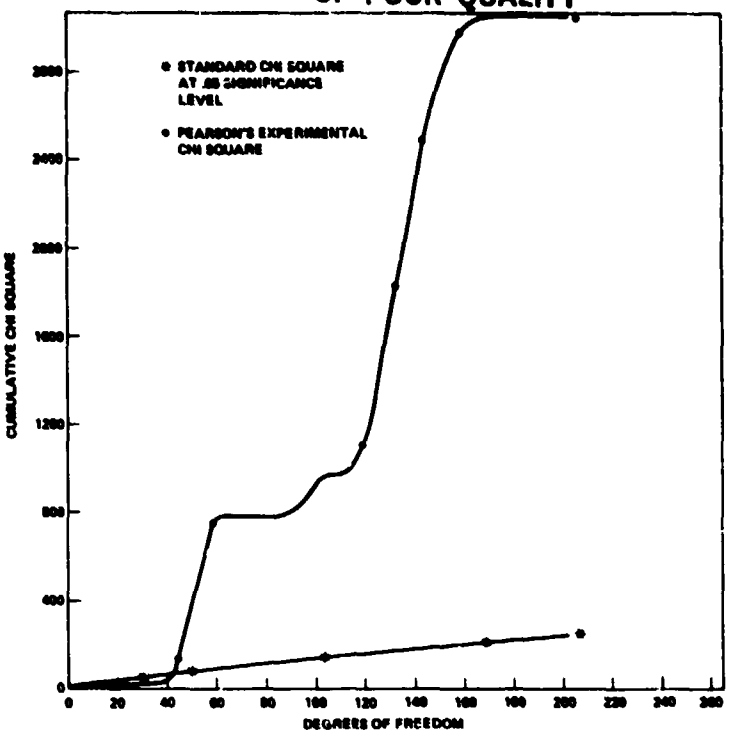


Figure 37. Chi square versus point number (nominally months) 13-month Lagrangian-smoothed flux (extended by derivative and connected to median cycle from max.) 1 coefficient linear model using cycles 1 through 17 predicting cycles 18 and 19 from point 2.

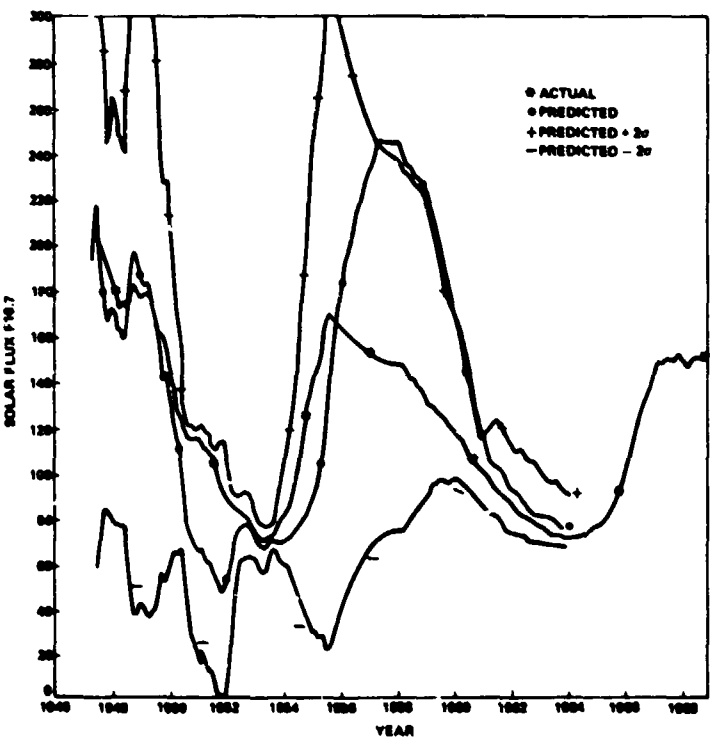


Figure 38. Predicted and actual flux versus time 13-month Lagrangian-smoothed flux (extended by derivative and connected to median cycle from max.) 1 coefficient linear model using cycles 1 through 17 predicting cycles 18 and 19 from point 2.

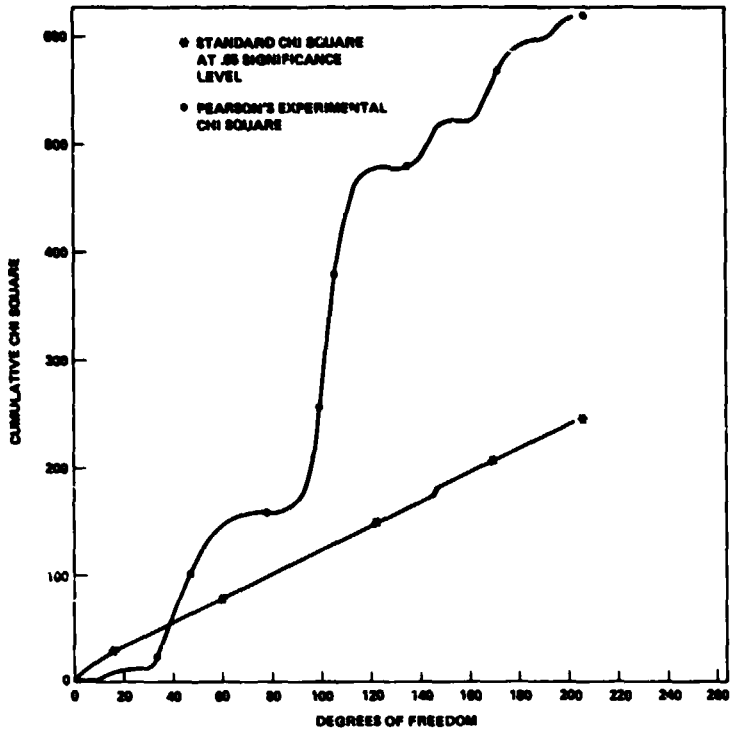


Figure 39. Chi square versus point number (nominally months) 13-month Lagrangian-smoothed flux (extended by derivative and connected to median cycle from max.) 1 coefficient linear model using cycles 1 through 18 predicting cycles 19 and 20 from point 2.

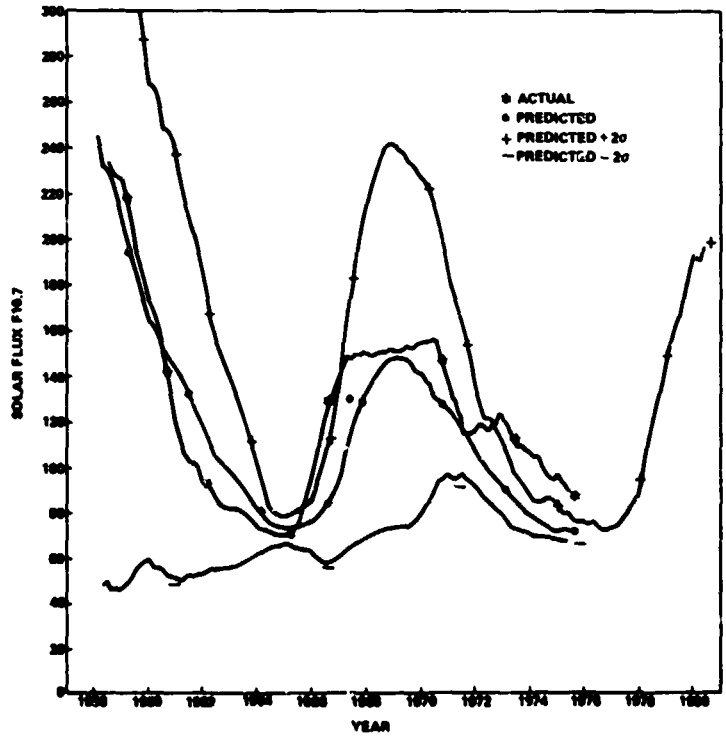


Figure 40. Predicted and actual flux versus time 13-month Lagrangian-smoothed flux (extended by derivative and connected to median cycle from max.) 1 coefficient linear model using cycles 1 through 18 predicting cycles 19 and 20 from point 2.

TABLE 2. EXTENDED CYCLE $\chi^2$

| Method | 15 & 16 | 16 & 17 | 17 & 18 | 18 & 19 | 19 & 20 | $\chi^2(0.05)$ |
|---|---|---|---|---|---|---|
| Double-cycle | | | | | | |
| 1. McNish-Lincoln | 1891 | | 7597 | | 738 | 300 |
| From Point 12 | 1828 | | 7753 | | 1000 | 287 |
| From Point 24 | 1910 | | 8179 | | 912 | 274 |
| Double-cycle | | | | | | |
| 2. Lagrangian | 190 | | 4000 | | 650 | 300 |
| From point 12 | 204 | | 3521 | | 643 | 287 |
| From point 24 | 213 | | 3075 | | 383 | 274 |
| Lagrangian | | | | | | |
| 3. Patched at min. | 214 | 426 | 1427 | 3306 | 454 | 242 |
| From point 12 | 175 | 425 | 1344 | 3371 | 514 | 229 |
| From point 24 | 181 | 439 | 1051 | 3250 | 459 | 216 |
| Lagrangian | | | | | | |
| 4. Patched at max. | 238 | 351 | 1348 | 3074 | 479 | 242 |
| From point 12 | 218 | 355 | 1243 | 3104 | 597 | 229 |
| From point 24 | 227 | 362 | 1155 | 2549 | 634 | 216 |
| Lagrangian | | | | | | |
| 5. Iterated | 248 | 676 | 2562 | 2406 | 348 | 242 |
| From point 12 | 207 | 728 | 2216 | 2355 | 686 | 229 |
| From point 24 | 231 | 653 | 1589 | 725 | 1038 | 216 |
| Lagrangian | | | | | | |
| 6. Derivative | 244 | 381 | 1430 | 3057 | 617 | 242 |
| From point 12 | 255 | 344 | 1312 | 2804 | 727 | 229 |
| From point 24 | 248 | 340 | 1249 | 2714 | 435 | 216 |

## V. CONSTRUCTION OF MODEL DATA BASE

The NASA-Marshall Space Flight Center solar activity long-range statistical estimation technique utilizes the 13-month Zurich procedure smoothed values of solar flux ($\bar{F}_{10.7}$) as the data base. For the period from August 1947 to the present, the actual measured values of solar flux, smoothed by the Zurich procedure, are used in the program. Prior to 1947, the solar flux was estimated using available Zurich sunspot numbers according to the procedure presented in Section II of this report. The estimated data plus actual measured data are then used in the main linear regression program to predict the remainder of the current cycle (peak-to-peak or minimum-to-minimum depending on initialization point), including the statistical confidence bounds, 97.7 and 2.3 percentile values. Table 3 provides a summary of the data base characteristics.

TABLE 3. FLUX

| Cycle | Year of Minimum | Year of Maximum | Rise Time In Years | Fall Time In Years | Min to Min Period | Max to Max Period |
|---|---|---|---|---|---|---|
| 0 | 1745 | 1750.3 | 5.3 | 4.9 | 10.2 | 11.2 |
| 1 | 1755.2 | 1761.5 | 6.3 | 5.0 | 11.3 | 8.2 |
| 2 | 1766.5 | 1769.7 | 3.2 | 5.8 | 9.0 | 8.7 |
| 3 | 1775.5 | 1778.4 | 2.9 | 6.3 | 9.2 | 9.7 |
| 4 | 1784.7 | 1783.1 | 3.4 | 10.2 | 13.6 | 17.1 |
| 5 | 1798.3 | 1805.2 | 6.9 | 5.4 | 12.3 | 11.2 |
| 6 | 1810.6 | 1816.4 | 5.8 | 6.9 | 12.7 | 13.5 |
| 7 | 1823.3 | 1829.9 | 6.6 | 4.0 | 10.6 | 7.3 |
| 8 | 1833.9 | 1837.2 | 3.3 | 6.3 | 9.6 | 10.9 |
| 9 | 1843.5 | 1848.1 | 4.6 | 7.9 | 12.5 | 12.0 |
| 10 | 1856.0 | 1860.1 | 4.1 | 7.1 | 11.2 | 10.5 |
| 11 | 1867.2 | 1870.6 | 3.4 | 8.3 | 11.7 | 13.3 |
| 12 | 1878.9 | 1883.9 | 5.0 | 5.7 | 10.7 | 10.2 |
| 13 | 1889.6 | 1894.1 | 4.5 | 7.6 | 12.1 | 12.9 |
| 14 | 1901.7 | 1907.0 | 5.3 | 6.6 | 11.9 | 10.6 |
| 15 | 1913.6 | 1917.6 | 4.0 | 6.0 | 10.0 | 10.8 |
| 16 | 1923.6 | 1928.4 | 4.8 | 5.4 | 10.2 | 9.0 |
| 17 | 1933.8 | 1937.4 | 3.6 | 6.7 | 10.3 | 10.3 |
| 18 | 1944.1 | 1947.7 | 3.6 | 6.5 | 10.1 | 10.5 |
| 19 | 1954.2 | 1958.2 | 4.0 | 6.4 | 10.4 | 12.4 |
| 20 | 1964.6 | 1970.6 | 6.0 | 5.8 | 11.8 | |
| 21 | 1976.4 | | | | | |
| STD. Deviation σ | | | 1.2 | 1.34 | 1.23 | 2.2 |
| 21 Cycle Average | | | | 6.4 | 11.02 | 11.02 |
| 20 Cycle Average | | | 4.6 | | | |
| Interpolation Points | | | 53 | 79 | | |

## VI. SMOOTHED PERIOD AND AMPLITUDE VARIATION

Using the sunspot periods obtained from Waldmeier [13], Chernosky and Hagan [14], or Schove [15], Table 3 was constructed up to 1947. Beyond 1947, actual flux observations were used. A five-cycle smoothing of these periods, rise times and fall times versus cycle number, is given in Figures 41 and 42. Figure 43 gives the five-cycle smoothed maximum amplitudes. These curves suggest a seven- to eight-cycle variation in the periods as well as the maximum amplitudes.

To further study this variation, autocorrelation and power spectrum analyses were run. Figures 44 and 45 give the results. It should be pointed out that these were determined from the Lagrangian interpolated data. This explains the rather regular variation at 132-point intervals on the autocorrelation and the sharp spike at 1/132 frequency on the power spectrum.

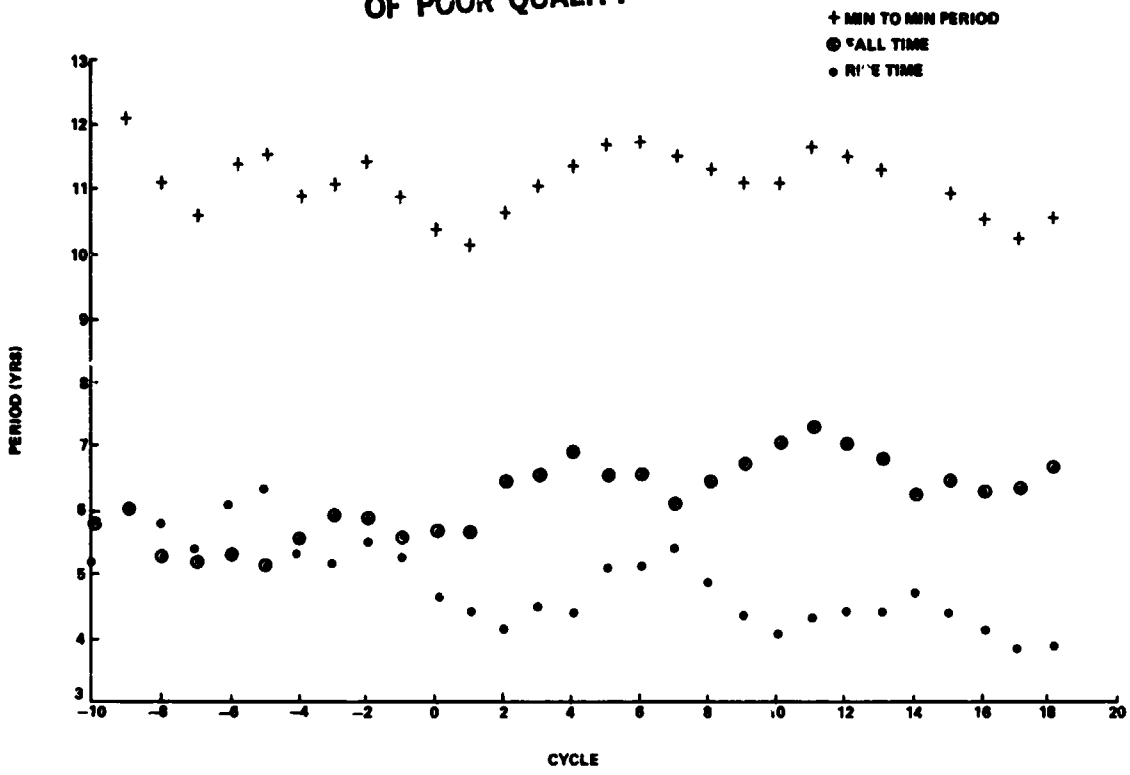


Figure 41. 5-cycle smooth periods (min. to min.), 0 cycle = year 1745 min and year 1750.3 max.

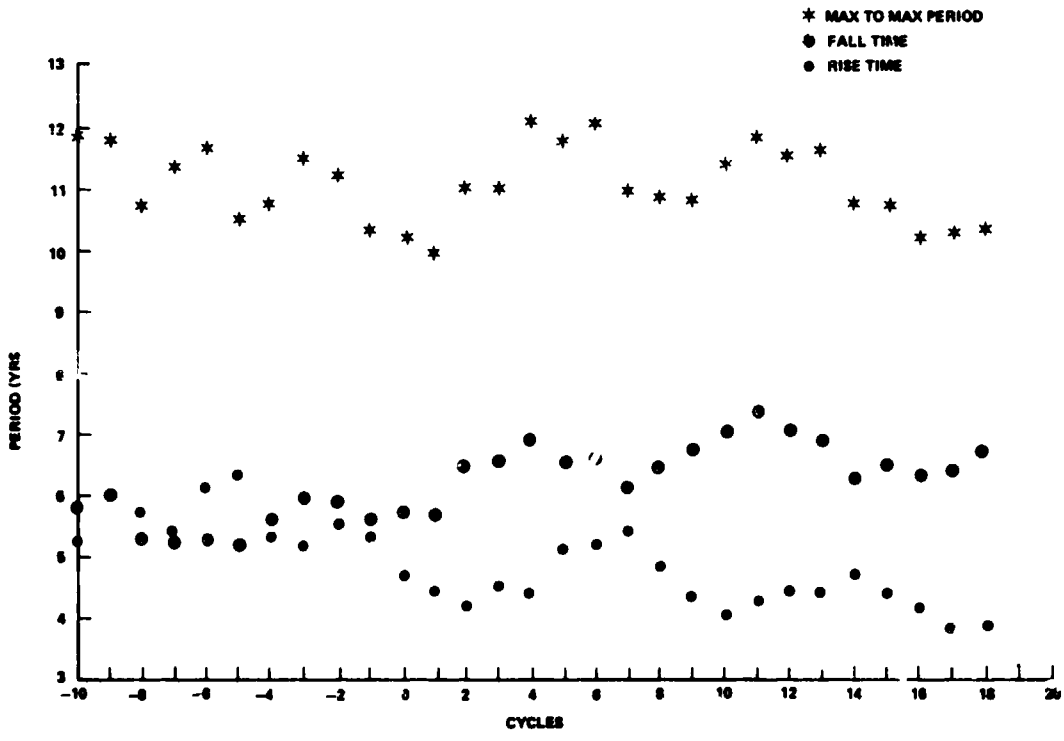


Figure 42. 5-cycle smooth periods (max. to max.), 0 cycle = year 1745 min and year 1750.3 max.

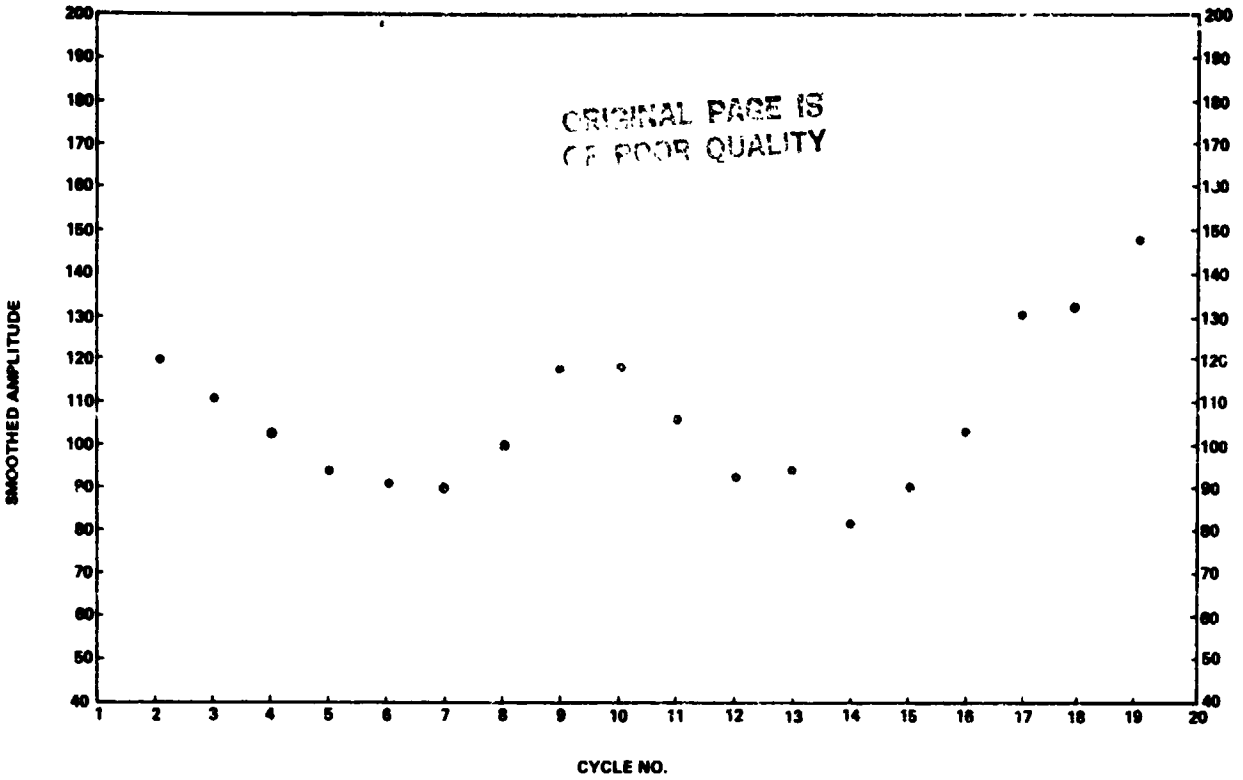


Figure 43. 5-cycle smoothed sunspot amplitude of 13-month smoothed monthly values.

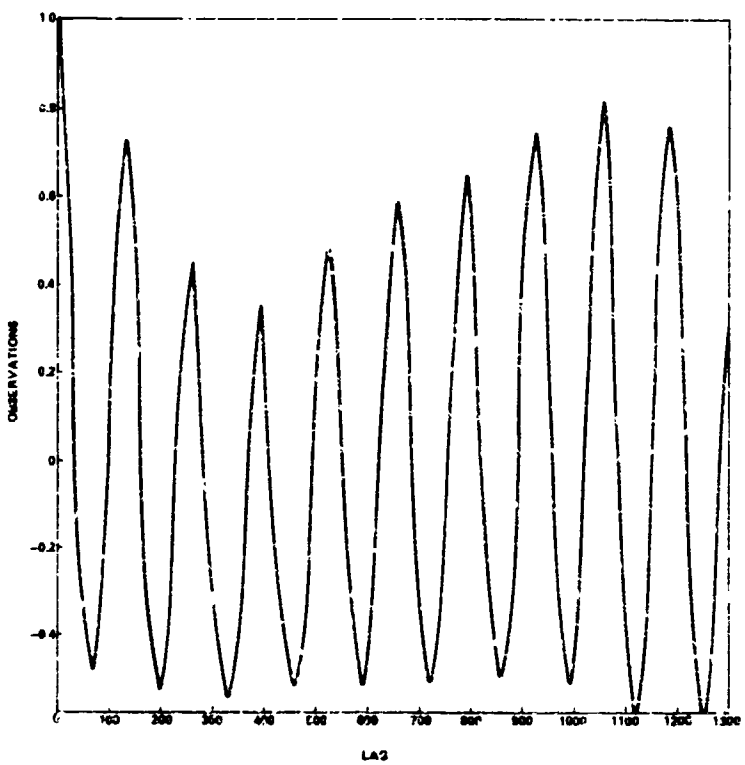


Figure 44. Autocorrelation of Lagrangian-smooth flux from cycles 1 through 20.

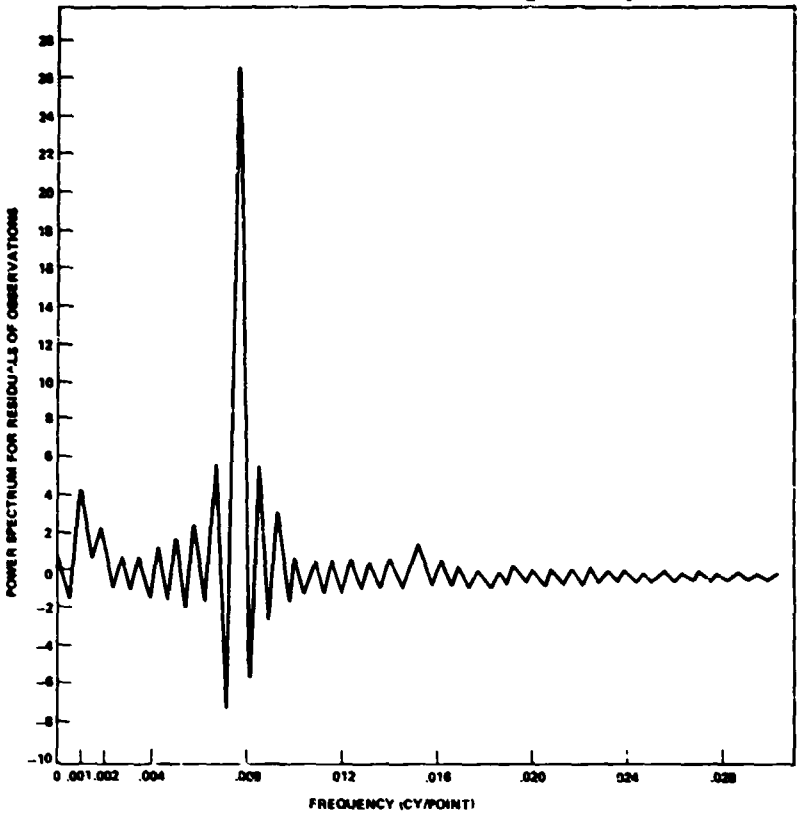


Figure 45. Power spectrum of cycles 1 through 20 Lagrangian-smooth flux.

Even though the Lagrangian interpolated data forced the preceding variations, it did not force the long-term variation (eight cycles) in the autocorrelation or the lower frequency peak at 0.0011 in the power spectrum. This gives some evidence to support the application of a correction to the average period for future predictions.

The following examples use the apparent systematic variation in the periods in Figures 41 and 42 to project the maximum to minimum fall time for cycle 21 and the maximum to maximum period for the same cycle.

Maximum to Minimum Fall Time--Cycle 21:

From Figure 41 the five-cycle smoothed fall time for cycle 19 is $\simeq$ 6.5 years. Now, if the last four fall times for cycles 17, 18, 19, and 20 plus the unknown fall time for cycle 21 are averaged and equated to the extrapolated smoothed fall time (7 years), we can then solve for the unknown fall time for cycle 21.

$$\frac{1}{5}(F_{17} + F_{18} + F_{19} + F_{20} + F_{21}) = \bar{F}_{19} \quad , \tag{7}$$

where

$F_{17}$ = 6.7 years (maximum to minimum period for cycle 17)

$F_{18}$ = 6.5 years

$F_{19}$ = 6.4 years

$F_{20}$ = 5.8 years

$F_{21}$ = Unknown

$\bar{F}_{19}$ = 7 years (five-cycle smoothed period at midpoint of smoothing interval).

From Eq. (7) one can now solve for $F_{21}$; i.e.,

$$F_{21} = 5\bar{F}_{19} - (F_{17} + F_{18} + F_{19} + F_{20})$$

$$= 5(6.5) - (6.7 + 6.5 + 6.4 + 5.8),$$

or

$F_{21}$ = 7.1 years maximum to minimum.

Minimum to Maximum Rise Time—Cycle 21-22:

Applying the same technique to the minimum to maximum rise times, the following results are obtained:

$R_{17}$ = 3.6

$R_{18}$ = 3.6

$R_{19}$ = 4.0

$R_{20}$ = 6.0

$R_{21}$ = Unknown

$\bar{R}_{19}$ = 4.5

$$R_{21} = 5(\bar{R}_{19}) - (R_{17} + R_{18} + R_{19} + R_{20})$$

$$= 5(4.5) - (3.6 + 3.6 + 4.0 + 6.0),$$

or

$R_{21}$ = 5.3 years minimum to maximum period.

## VII. COMPUTER PROGRAMS

The computer programs to calculate the predicted cycles and perform subsequent statistical analysis were developed by Computer Sciences Corporation under contract NAS 8-31640. The programs were implemented in FORTRAN on the UNIVAC 1100/80 computer at Marshall Space Flight Center.

Although six distinct program versions were used to obtain the numerical results of Table 2, all programs were essentially variations on the single theme of linear regression. Gaussian reduction was used to solve the normal equations via subroutine GJR, contained in the UNIVAC "Math-Pack" subroutine library. The evaluation of the inverse $\chi^2$ function was accomplished through subroutine CHIN (also drawn from the "math-pack") and through normal approximation for large degrees-of-freedom. Graphic output was performed off-line on an FR-80 micrographics unit.

Space prohibits including listings for all six programs. However, FORTRAN source code for the Lagrangian prediction connected at cycle maximum appears in Appendix C. All of the system subroutines are not listed but, rather, only the main program and the McNish-Lincoln subroutine described in Appendix A.

## VIII. APPLICATIONS FOR SPACE PROGRAM DESIGN AND MISSION ANALYSIS

The solar flux and geomagnetic activity are principal inputs to the upper atmosphere models and thus the ambient density values computed for use in spacecraft orbital lifetime estimation control analyses programs. For those spacecraft projects which require a design lifetime at a given orbital altitude(s) and/or a specified control capability, it is recommended that the 97.7 percentile estimates of solar and geomagnetic activity be used. This then permits the design of a statistically conservative spacecraft lifetime at a given orbital altitude(s). It can be interpreted to mean the spacecraft will have a 97.7 percent chance of (1) remaining in orbit for at least the number of months calculated by the orbital lifetime scheme and/or (2) maintaining the specified control capability. The determination should be made based upon the most current long range statistical estimate of the solar flux and geomagnetic index consistent with the critical project development decision time points prior to launch of the spacecraft.

For spacecraft already in orbit, or for some prelaunch orbital altitude tradeoff analyses, the 97.7, 50, and 2.3 percentile values may be used to compute the respective expected future lifetimes and control capability and then a statistical interpolation made as a first estimate of the probability that (1) the spacecraft will remain in orbit, or above a given orbital altitude, for any selected time period or (2) the specified control capability will be maintained for the required time in orbit.

After launch, the statements on remaining lifetime should always be given in terms of the probability that a spacecraft's lifetime will equal or exceed a given date or dates depending on program management requirements.

Since orbital lifetime programs and control analyses require a specific date to associate with the solar flux $F_{10.7}$ and geomagnetic $A_p$ estimations to compute a corresponding atmospheric density, the data points should be identified with the midway point of the given month.

It should be recognized and remembered that all statements of spacecraft orbital lifetime and control capabilities made using inputs of expected solar activity to the upper atmosphere models, must be interpreted in terms of statistical probabilities. Figure 46 provides a description of the various inputs necessary to compute a spacecraft's orbital lifetime.

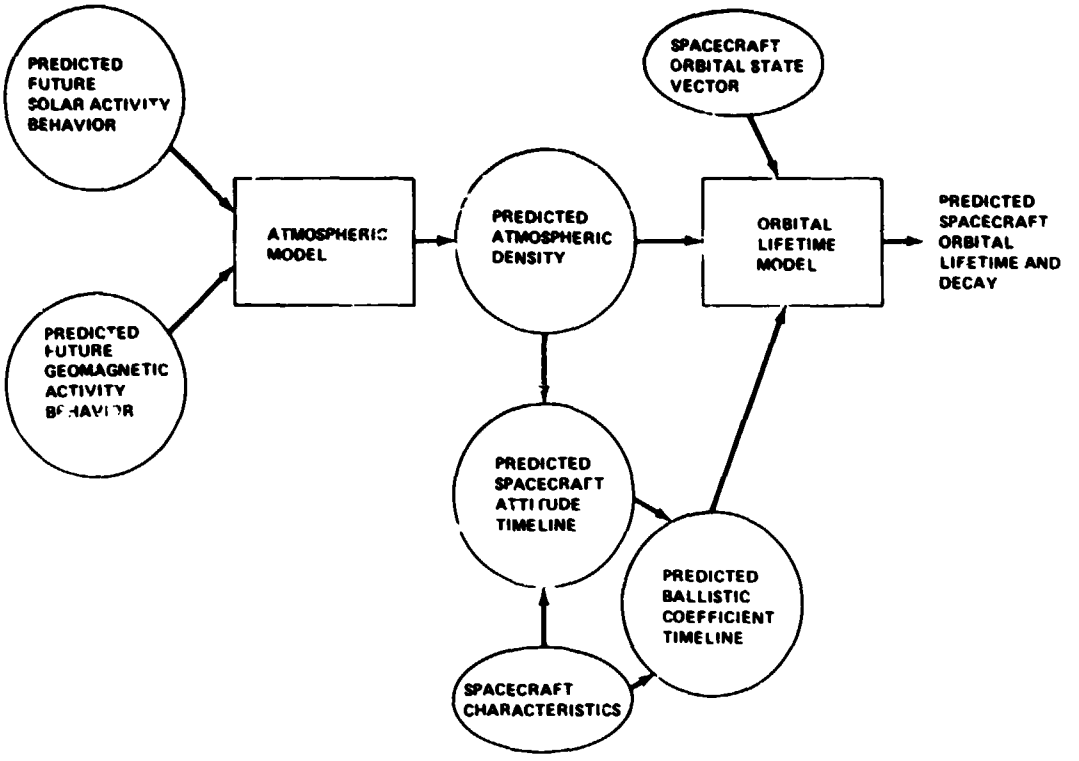


Figure 46. Solar predictions and spacecraft orbital lifetime.

## IX. CONCLUSIONS

The results of this study strongly suggest that better predictions are possible, in a chi-square sense, by "lining up" the maximums (or minimums, or both).

Evidence has also been presented which supports the existence of an aperiodic variation in the periods as well as in the amplitudes.

# APPENDIX A

## Least Squares Development

The expected value of R (solar flux) at k points beyond m, where m is the number of points known (or used as known) in the current cycle and k is the number of points beyond m, is:

$$R_{m+k,j} = \bar{R}_{m+k} + \sum_{q=1}^{m} (C_{q,k}\ \Delta R_{q,j} + b_{q,k}\ \Delta \dot{R}_{q,j}) \quad , \tag{A-1}$$

where

$$\bar{R}_{m+k} = \frac{1}{N} \sum_{j=1}^{N} R_{m+k,j} \qquad ; \qquad N = \text{Number of known past cycles} \tag{A-2}$$

$$\Delta R_{m+k,j} = R_{m+k,j} - \bar{R}_{m+k} \quad . \tag{A-3}$$

Then Eq. (A-1) may be written as

$$\Delta R_{m+k,j} = \sum_{q=1}^{m} (C_{q,k} \Delta R_{q,j} + b_{q,k} \Delta \dot{R}_{q,j}). \tag{A-4}$$

Then

$$\Delta \dot{R}_{q,j} = \frac{1}{2\Delta t_j} [\Delta R_{q+1,j} - \Delta R_{q-1,j}] \tag{A-5}$$

$$\Delta R_{m+k,j} = \sum_{q=1}^{m} (C_{q,k}\ \Delta R_{q,j} + b_{q,k}\ \Delta \dot{R}_{q,j}) \quad . \tag{A-6}$$

The sum of the deviations squared is then

$$S = \sum_{j=1}^{N} \left[ \Delta R_{m+k,j} - \sum_{q=1}^{m} (C_{q,k}\ \Delta R_{q,j} + b_{q,k}\ \Delta \dot{R}_{q,j}) \right]^2 \tag{A-7}$$

$$\frac{\partial S}{\partial C_{pk}} = 2 \sum_{j=1}^{N} \left[ \Delta R_{m+k,j} - \sum_{q=1}^{m} C_{q,k}\ \Delta R_{q,j} + b_{q,k}\ \Delta \dot{R}_{q,j} \right] \Delta R_{p,j} \tag{A-8}$$

$$\frac{\partial s}{\partial b_{pk}} = 2 \sum_{j=1}^{N} \left[ \Delta R_{m+k,j} - \sum_{q=1}^{m} C_{q,j}\ \Delta R_{q,j} + b_{q,k}\ \Delta \dot{R}_{q,j} \right] \Delta \dot{R}_{p,j} \quad . \tag{A-9}$$

This equated to zero gives the normal equations

$$\sum_{j=1}^{N} \Delta R_{m+k,j}\, \Delta R_{p,j} = \sum_{j=1}^{N} \sum_{q=1}^{m} C_{q,k}\, \Delta R_{q,j}\, \Delta R_{p,j} + \sum_{j=1}^{N} \sum_{q=1}^{m} b_{q,k}\, \Delta \dot{R}_{q,j} \Delta R_{p,j} \tag{A-10}$$

$$\sum_{j=1}^{N} \Delta R_{m+k,j}\, \Delta \dot{R}_{p,j} = \sum_{j=1}^{N} \sum_{q=1}^{m} C_{q,k}\, \Delta R_{q,j}\, \Delta \dot{R}_{p,j} + \sum_{j=1}^{N} \sum_{q=1}^{m} b_{q,k}\, \Delta \dot{R}_{q,j}\, \Delta \dot{R}_{p,j} . \tag{A-11}$$

Note:

$$\Delta \dot{R}_{q,j} = \frac{1}{2\Delta t_j} [\Delta R_{q+1,j} - \Delta R_{q-1,j}] \tag{A-12}$$

$$\Delta t_j = \frac{P_j}{\bar{P}} \; ; \quad \bar{P} = \frac{1}{N} \sum_{j=1}^{N} P_j . \tag{A-13}$$

For one-point prediction, p = 1, m = 1.

$$\sum_{j=1}^{N} \Delta R_{k+1,j}\, \Delta R_{1j} = \sum_{j=1}^{N} C_{1k}\, \Delta R_{1j}\, \Delta R_{1j} + \sum_{j=1}^{N} b_{1k}\, \Delta \dot{R}_{1j}\, \Delta R_{1j} \tag{A-14}$$

$$\sum_{j=1}^{N} \Delta R_{k+1,j}\, \Delta \dot{R}_{p,j} = \sum_{j=1}^{N} C_{1k}\, \Delta R_{1j}\, \Delta \dot{R}_{1j} + \Sigma b_{1k}\, \Delta \dot{R}_{1j}\, \Delta \dot{R}_{1j} . \tag{A-15}$$

Since the C's and b's are not summed, they may be taken outside the summation; i.e.,

$$C_{1k}\ \Sigma \Delta R_{1j}\, \Delta R_{1j} + b_{1k}\ \Sigma \Delta \dot{R}_{1j}\, \Delta R_{1j} = \Sigma \Delta R_{k+1,j}\, \Delta R_{1j} \tag{A-16}$$

$$C_{1k}\ \Sigma \Delta R_{1j}\, \Delta \dot{R}_{1j} + b_{1k}\ \Sigma \Delta \dot{R}_{1k}\, \Delta \dot{R}_{1j} = \Sigma \Delta R_{k+1,j}\, \Delta \dot{R}_{1j} . \tag{A-17}$$

This can be written in vector and matrix notation if we let

$$B = \begin{pmatrix} \Sigma \Delta R_{k+1,j}\, \Delta R_{1j} \\ \Sigma \Delta R_{k+1,j}\, \Delta \dot{R}_{1j} \end{pmatrix} \tag{A-18}$$

$$A = \begin{pmatrix} \Sigma \Delta R_{1j}\, \Delta R_{1j} & \Sigma\, \Delta \dot{R}_{1j}\, \Delta R_{1j} \\ \Sigma \Delta R_{1j}\, \Delta \dot{R}_{1j} & \Sigma\, \Delta \dot{R}_{1j}\, \Delta \dot{R}_{1j} \end{pmatrix} \tag{A-19}$$

$$C = \begin{pmatrix} C_{1k} \\ b_{1k} \end{pmatrix} . \qquad \text{(A-20)}$$

Then $AC = B \rightarrow C = A^{-1} B$.

For two-point prediction

$$\Sigma\Delta R_{2+k,j}\Delta R_{1j} = \Sigma C_{1k}\Delta R_{1j}\Delta R_{1j} + \Sigma C_{2k}\Delta R_{2j}\Delta R_{1j} + \Sigma b_{1k}\Delta \dot{R}_{1j}\Delta R_{1j} + \Sigma b_{2k}\Delta \dot{R}_{2j}\Delta R_{1j} \quad \text{(A-21)}$$

$$\Sigma\Delta R_{2+k,j}\Delta R_{2j} = \Sigma C_{1k}\Delta R_{1j}\Delta R_{2j} + \Sigma C_{2k}\Delta R_{2j}\Delta R_{2j} + \Sigma b_{1k}\Delta \dot{R}_{1j}\Delta R_{2j} + \Sigma b_{2k}\Delta \dot{R}_{2j}\Delta R_{2j} \quad \text{(A-22)}$$

$$\Sigma\Delta R_{2+k,j}\Delta \dot{R}_{1j} = \Sigma C_{1k}\Delta R_{1j}\Delta \dot{R}_{1j} + \Sigma C_{2k}\Delta R_{2j}\Delta \dot{R}_{1j} + \Sigma b_{1k}\Delta \dot{R}_{1j}\Delta \dot{R}_{1j} + \Sigma b_{2k}\Delta \dot{R}_{2j}\Delta \dot{R}_{1j} \quad \text{(A-23)}$$

$$\Sigma\Delta R_{2+k,j}\Delta \dot{R}_{2j} = \Sigma C_{1k}\Delta R_{1j}\Delta \dot{R}_{2j} + \Sigma C_{2k}\Delta R_{2j}\Delta \dot{R}_{2j} + \Sigma b_{1k}\Delta \dot{R}_{1j}\Delta \dot{R}_{2j} + \Sigma b_{2k}\Delta \dot{R}_{2j}\Delta \dot{R}_{2j} \quad \text{(A-24)}$$

This may be written in vector and matrix notation if we let

$$B = \begin{pmatrix} \Sigma\Delta R_{2+k,j}\ \Delta R_{1j} \\ \Sigma\Delta R_{2+k,j}\ \Delta R_{2j} \\ \Sigma\Delta R_{2+k,j}\ \Delta \dot{R}_{1j} \\ \Sigma\Delta R_{2+k,j}\ \Delta \dot{R}_{2j} \end{pmatrix} \quad , \text{ where } \Sigma \equiv \sum_{j=1}^{N} \qquad \text{(A-25)}$$

$$A = \begin{pmatrix} \Sigma\Delta R_{1j}\ \Delta R_{1j} & \Sigma\Delta R_{2j}\ \Delta R_{1j} & \Sigma\Delta \dot{R}_{1j}\ \Delta R_{1j} & \Sigma\Delta \dot{R}_{2j}\ \Delta R_{1j} \\ \Sigma\Delta R_{1j}\ \Delta R_{2j} & \Sigma\Delta R_{2j}\ \Delta R_{2j} & \Sigma\Delta \dot{R}_{1j}\ \Delta R_{2j} & \Sigma\Delta \dot{R}_{2j}\ \Delta R_{2j} \\ \Sigma\Delta R_{1j}\ \Delta \dot{R}_{1j} & \Sigma\Delta R_{2j}\ \Delta \dot{R}_{1j} & \Sigma\Delta \dot{R}_{1j}\ \Delta \dot{R}_{1j} & \Sigma\Delta \dot{R}_{2j}\ \Delta \dot{R}_{1j} \\ \Sigma\Delta R_{1j}\ \Delta \dot{R}_{2j} & \Sigma\Delta R_{2j}\ \Delta \dot{R}_{2j} & \Sigma\Delta \dot{R}_{1j}\ \Delta \dot{R}_{2j} & \Sigma\Delta \dot{R}_{2j}\ \Delta \dot{R}_{2j} \end{pmatrix} \qquad \text{(A-26)}$$

$$C = \begin{pmatrix} C_{1k} \\ C_{2k} \\ b_{1k} \\ b_{2k} \end{pmatrix} \qquad \text{(A-27)}$$

Then $AC = B \rightarrow C = A^{-1} B$. (A-28)

## APPENDIX B

### Cubic Connection From Predicted To Mean Cycle

1) Select the last inflection point of the predicted cycle $(t_I, F_I)$ near the 24-month point before the maximum. This should be done with at least a five-point numerical scheme for determining where the second derivative goes to zero. One such scheme is Sterling's [16]

$$\left(\frac{d^2F}{dt^2}\right)_N = \frac{1}{(\Delta t)^2}\left[-\frac{F_{N+2}}{12} + \frac{4F_{N+1}}{3} - \frac{5F_N}{2} + \frac{4F_{N-1}}{3} - \frac{F_{N-2}}{12}\right]. \qquad (B\text{-}1)$$

2) Select the maximum (or minimum) on the mean cycle $(t_m, F_m)$. This is normally input, but it can also be determined numerically.

$$\left(\frac{dF}{dt}\right)_N = \frac{1}{\Delta t}\left[-\frac{1}{12}F_{N+2} + \frac{2}{3}F_{N+1} - \frac{2}{3}F_{N-1} + \frac{1}{12}F_{N-2}\right]. \qquad (B\text{-}2)$$

The second derivative should be zero at $(t_I, F_I)$, and the first derivative is zero at $(t_m, F_m)$. A cubic curve is the lowest degree polynomial which can be determined that will go through the two points and have these properties at the two points.

The coefficients of the polynomial

$$F = at^3 + bt^2 + ct + d \qquad (B\text{-}3)$$

are to be determined from the following four linear equations and will have the required four properties:

$$6at_I + 2b = 0 \quad \left\{\begin{array}{l}\text{second derivative is zero at}\\ \text{inflection point}\end{array}\right. \qquad (B\text{-}4)$$

$$3at_m^2 + 2bt_m + c = 0 \quad \left\{\begin{array}{l}\text{first derivative is zero at}\\ \text{maximum or minimum}\end{array}\right. \qquad (B\text{-}5)$$

$$at_I^3 + bt_I^2 + ct_I + d = F_I \quad \left\{\begin{array}{l}\text{curve goes through the inflection}\\ \text{point } (t_I, F_I)\end{array}\right. \qquad (B\text{-}6)$$

$$at_m^3 + bt_m^2 + ct_m + d = F_m \quad \left\{\begin{array}{l}\text{curve goes through the maximum}\\ \text{(or minimum) point } (t_m, F_m).\end{array}\right. \qquad (B\text{-}7)$$

These four linear equations in the four coefficients are to be solved for a, b, c, and d. The solutions are:

$$b = \frac{F_m - F_I}{-2t_m^2 + \frac{2}{3}\frac{t_m^3}{t_I} - \frac{2}{3}t_I^2 + 2t_m t_I} \tag{B-8}$$

$$a = -\frac{1}{3t_I} b \tag{B-9}$$

$$c = -\left(2t_m - \frac{t_m^2}{t_I}\right) b \tag{B-10}$$

$$d = F_I - \left(\frac{2}{3}t_I^2 - 2t_m t_I + t_m^2\right) b \quad . \tag{B-11}$$

# APPENDIX C
## Computer Program Listings

```
      INTEGER TITLE(12),PCYC1,PCYC2,CASE
      DIMENSION EPOCH(21),PERIOD(21),R(132,21),RMEAN(264),
     $  RPRED(264),YEAR(264),ROBSV(264),ERRUP(264),ERRDN(264),
     $  CHIPRS(264),CHITAB(264),DGFREE(264)
      INCLUDE PLOT1,LIST
PLOT1   PROC
      DIMENSION ITITL1(12),ITITL2(12),ITITL3(12),ITITL4(12)
      DIMENSION ICAP1(13),ICAP2(17),ICAP4(10),INSTR(22)
      DATA INSTR/30HFICHE AND ONE HARDCOPY. THANKS,17*6H      /
      DATA ITITL1/6HYEAR  ,11*6H      /
      DATA ITITL2/18HSOLAR FLUX F10.7  ,9*6H      /
      DATA ITITL3/18HDEGREES OF FREEDOM,9*6H      /
      DATA ITITL4/24HCUMULATIVE CHI SQUARE   ,8*6H      /
      DATA ICAP1/36H'*' DENOTES ACTUAL '.' DENOTES NOMIN,
     $           42HAL '+','-' DENOTE +2 SIGMAS,-2 SIGMAS     /
      DATA ICAP4/30H'*' DENOTES THEORETICAL '.' DE,
     $           30HNOTES EXPERIMENTAL (PEARSON'S)/
      DATA IASTR/40/,IDOT/35/,IPLUS/34/,IMINUS/33/
 1000 FORMAT(I3,' COEFFICIENT LINEAR MODEL USING CYCLES ',I2,
     $  ' THROUGH ',I2,' PREDICTING CYCLES ',I2,' AND ',I2,
     $  ' FROM POINT ',I3,4X)
      CALL IDENT(105,INSTR)
 END
      READ(5,5000) TITLE
      READ(5,5005) M,N
      READ(5,5010) (EPOCH(J),J=1,N)
      DO 5 J=1,N
      READ(5,5015) PERIOD(J)
      READ(5,5020) (R(I,J),I=1,M)
    5 CONTINUE
      READ(5,5025) NCASES
      DO 900 CASE=1,NCASES
      READ(5,5030) NU1,NU2,MU,MU2,ALPHA
      PCYC1 = NU2 + 1
      PCYC2 = NU2 + 2
      DO 10 K=1,M
      ROBSV(K) = R(K,PCYC1)
      ROBSV(M+K) = R(K,PCYC2)
      YEAR(K) = EPOCH(PCYC1) + (K-1)*(PERIOD(PCYC1)/M)
      YEAR(M+K) = EPOCH(PCYC2) + (K-1)*(PERIOD(PCYC2)/M)
   10 CONTINUE
      CALL LINCMC(R,M,N,NU1,NU2,MU,MU2,RMEAN,RPRED,ERRUP,ERRDN)
      INCLUDE C1,LIST
C1      PROC
      CALL PCHMAX(RPRED,ERRUP,ERRDN,M,INFL,NPTS)
      MM = M + NPTS
 END
      WRITE(6,6000) TITLE,MU,NU1,NU2,MU2,PCYC1,PCYC2
      WRITE(6,6005) ALPHA
      DO 20 K=1,MU2
      WRITE(6,6010) YEAR(K),ROBSV(K),RMEAN(K)
   20 CONTINUE
      MU2P1 = MU2 + 1
      CHIPR = 0.
      INCLUDE C2,LIST
C2      PROC
```

```
      DO 70 K=MU2P1,MM
      IF(K .GT. INFL) GO TO 30
      DEV = RPRED(K) - RMEAN(K)
   30 CHIPR = CHIPR + (RPRED(K) - ROBSV(K))**2/RPRED(K)
      CHIPRS(K) = CHIPR
      NDF = K - MU2
      DGFREE(K) = NDF
      CHITAB(K) = CHIN(ALPHA,NDF,$40)
      GO TO 50
   40 CHITAB(K) = 0.5*(SQRT(2.*DGFREE(K) - 1.) + 1.9602)**2
   50 IF(K .GT. INFL) GO TO 60
      WRITE(6,6015) YEAR(K),ERRUP(K),ROBSV(K),RPRED(K),ERRDN(K),
     $  RMEAN(K),DEV,CHIPRS(K),CHITAB(K),NDF
      GO TO 70
   60 WRITE(6,6020) YEAR(K),ERRUP(K),ROBSV(K),RPRED(K),ERRDN(K),
     $CHIPRS(K),CHITAB(K),NDF
      IF(K .LT. M) WRITE(6,6025)
   70 CONTINUE
 END
      INCLUDE PLOT2,LIST
PLOT2   PROC
      XMIN = FLOAT(IFIX(YEAR(1) - 1.))
      XMAX = FLOAT(IFIX(YEAR(2*M) + 1.))
      XMID = (XMIN + XMAX)/2.
      NP = MM - MU2P1 + 1
      CALL SETMIV(24,24,120,24)
      CALL GRID1V(3,XMIN,XMAX,0.,300.,.5,5.,-2,-2,-4,-4,4,3)
      CALL XSCLV1(XMIN,IXMIN,IERR)
      CALL YSCLV1(150.,IYMID,IERR)
      IX = IXMIN - 40
      IY = IYMID + 90
      CALL APRNTV(0.-12,16,ITITL2,IX,IY)
      CALL XSCLV1(XMID,IXMID,IERR)
      CALL YSCLV1(0.,IYMIN,IERR)
      IX = IXMID - 12
      IY = IYMIN - 24
      CALL PRINTV(4,ITITL1,IX,IY)
      IX = IXMID - 312
      IY = IY - 25
      CALL PRINTV(78,ICAP1,IX,IY)
      IX = IXMID - 288
      IY = IY - 15
      CALL PRINTV(72,TITLE,IX,IY)
      ENCODE(102,1000,ICAP2) MU,NU1,NU2,PCYC1,PCYC2,MU2
      IX = IXMID - 408
      IY = IY - 15
      CALL PRINTV(102,ICAP2,IX,IY)
      CALL CHARSZ(18)
      CALL PLOTLN(-2*M,YEAR,ROBSV,IASTR)
      CALL PLOTLN(-NP,YEAR(MU2P1),RPRED(MU2P1),IDOT)
      CALL PLOTLN(-NP,YEAR(MU2P1),ERRUP(MU2P1),IPLUS)
      CALL PLOTLN(-NP,YEAR(MU2P1),ERRDN(MU2P1),IMINUS)
      CALL CHARSZ(14)
      YMAX = AMAX0(CHIPRS(MM),CHITAB(MM)) + 10.
      YMID = YMAX/2.
      CALL DXDYV(2,0.,YMAX,DY,MY,JY,NY,8.,IERR)
      CALL GRID1V(3,0.,264.,0.,YMAX,5.,DY,-4,-MY,-4,-JY,3,NY)
```

```
      CALL XSCLV1(0.,IXMIN,IERR)
      CALL YSCLV1(YMID,IYMID,IERR)
      IX = IXMIN - (NY+2)*8
      IY = IYMID + 138
      CALL APRNTV(0,-12,21,ITITL4,IX,IY)
      CALL XSCLV1(132.,IXMID,IERR)
      CALL YSCLV1(0.,IYMIN,IERR)
      IX = IXMID - 72
      IY = IYMIN - 24
      CALL PRINTV(18,ITITL3,IX,IY)
      IX = IXMID - 240
      IY = IY - 25
      CALL PRINTV(60,ICAP4,IX,IY)
      IX = IXMID - 288
      IY = IY - 15
      CALL PRINTV(72,TITLE,IX,IY)
      IX = IXMID - 408
      IY = IY - 15
      CALL PRINTV(102,ICAP2,IX,IY)
      CALL CHARSZ(18)
      CALL PLOTLN(-NP,DGFREE(MU2P1),CHITAB(MU2P1),IASTR)
      CALL PLOTLN(-NP,DGFREE(MU2P1),CHIPRS(MU2P1),IDOT)
      CALL CHARSZ(14)
      END
  900 CONTINUE
      CALL ENDJOB
      STOP
 5000 FORMAT(12A6)
 5005 FORMAT(2I4)
 5010 FORMAT(8F9.3)
 5015 FORMAT(4X,F5.1)
 5020 FORMAT(12F6.1)
 5025 FORMAT(I4)
 5030 FORMAT(4I4,F4.2)
 6000 FORMAT(1H1,12A6/1HO,I3,1X,'COEFFICIENT LINEAR MODEL USING CYCLES',
     $  1X,I2,1X,'THROUGH',1X,I2,1X,'FROM POINT',1X,I3,1X,'PREDICTING ',
     $  'CYCLES',1X,I2,1X,'AND',1X,I2)
 6005 FORMAT(1HO,T104,'PEARSON''S',5X,'CHI-SQUARE'/6X,'DATE',8X,'+2 SIGM
     $AS',5X,'OBSERVED',6X,'PREDICTED',5X,'-2 SIGMAS',4X,'MEAN CYCLE',
     $5X,'DEVIATION',5X,'CHI-SQUARE',4X,'SIGNIFICANCE'/1X,T102,
     $'(CUMULATIVE)',4X,'LEVEL=',F4.2//)
 6010 FORMAT(2X,F8.3,24X,F5.1,37X,F5.1)
 6015 FORMAT(2X,F8.3,10X,5(F5.1,9X),F5.1,2X,2(5X,F10.3),'(',I3,')')
 6020 FORMAT(2X,F8.3,10X,4(F5.1,9X),21X,2(5X,F10.3),'(',I3,')')
 6025 FORMAT(1H+,'*')
      END
```

ECAST-A

```
      SUBROUTINE LINCMC(R,M,N,NU1,NU2,MU,MU2,RMEAN,RPRED,ERRUP,ERRDN)
      INTEGER P,Q
      DIMENSION R(M,N),RMEAN(1),RPRED(1),ERRUP(1),ERRDN(1),
     $  DR(132,21),A(10,10),AINV(10,10),APRIME(100),B(132,10),
     $  C(132,10),JDUM(10),DETA(2)
      EQUIVALENCE (A(1,1),AINV(1,1),APRIME(1))
      MU1 = MU2 - MU + 1
      NU = NU2 - NU1 + 1
      MUPRIM = M - MU2
      DO 15 I=1,M
      RMEAN(I) = 0.
      DO 10 J=NU1,NU2
      RMEAN(I) = RMEAN(I) + R(I,J)
   10 CONTINUE
      RMEAN(I) = RMEAN(I)/NU
   15 CONTINUE
      DO 25 I=1,M
      DO 20 J=NU1,N
      DR(I,J) = R(I,J) - RMEAN(I)
   20 CONTINUE
   25 CONTINUE
      DO 40 K=1,MU
      DO 35 Q=1,MU
      A(K,Q) = 0.
```

```
      DO 30 J=NU1,NU2
      A(K,Q) = A(K,Q) + DR(MU1+K-1,J)*DR(MU1+Q-1,J)
   30 CONTINUE
   35 CONTINUE
   40 CONTINUE
      DO 55 P=1,NUPRIM
      DO 50 Q=1,MU
      B(P,Q) = 0.
      DO 45 J=NU1,NU2
      B(P,Q) = B(P,Q) + DR(MU2+P,J)*DR(MU1+Q-1,J)
   45 CONTINUE
   50 CONTINUE
   55 CONTINUE
      K = 0
      DO 65 J=1,MU
      DO 60 I=1,MU
      K = K + 1
      APRIME(K) = A(I,J)
   60 CONTINUE
   65 CONTINUE
      DETA(1) = 3.
      DETA(2) = 0.
      CALL GJR(A,MU,MU,MU,MU,$999,JDUM,DETA)
      IF(DETA(1) .EQ. 0.) GO TO 999
      K = MU*MU + 1
      DO 75 J=MU,1,-1
      DO 70 I=MU,1,-1
      K = K - 1
      AINV(I,J) = APRIME(K)
   70 CONTINUE
   75 CONTINUE
      DO 90 P=1,MUPRIM
      DO 85 K=1,MU
      C(P,K) = 0.
      DO 80 Q=1,MU
      C(P,K) = C(P,K) + B(P,Q)*AINV(Q,K)
   80 CONTINUE
   85 CONTINUE
   90 CONTINUE
      DO 105 P=1,M
      IF(P .GT. MU2) GO TO 95
      RPRED(P) = R(P,NU2+1)
      GO TO 105
   95 RPRED(P) = 0.
      DO 100 K=1,MU
      RPRED(P) = RPRED(P) + C(P-MU2,K)*DR(MU1+K-1,NU2+1)
  100 CONTINUE
      RPRED(P) = RPRED(P) + RMEAN(P)
  105 CONTINUE
      MU2P1 = MU2 + 1
      DO 120 P=MU2P1,M
      SIGMA = 0.
      DO 115 J=NU1,NU2
      SIGMA = SIGMA + (R(P,J) - RPRED(P))**2
```

```
115 CONTINUE
    SIGMA = SQRT(SIGMA/(NU-MU+1))
    ERRUP(P) = RPRED(P) + 2.*SIGMA
    ERRDN(P) = RPRED(P) - 2.*SIGMA
    IF(ERRDN(P) .LT. 0.) ERRDN(P) = 0.
120 CONTINUE
    RETURN
999 STOP SINGLR
    END
```

## REFERENCES


1. NASA Space Vehicle Design Criteria: Models of Earth's Atmosphere (90 to 2500 km). NASA SP-8021, National Aeronautics and Space Administration, Washington. D.C., 1973.

2. Jacchia, L. G.: New Static Models of the Thermosphere and Exosphere with Empirical Temperature Profiles. Special Report No. 313, Smithsonian Astrophysical Observatory, Cambridge, Massachusetts, 1970.

3. Jacchia, L. G.: Revised Static Models of the Thermosphere and Exosphere with Empirical Temperature Profiles. Special Report No. 332, Smithsonian Astrophysical Observatory, Cambridge, Massachusetts, 1971.

4. Jacchia, L. G.: Thermospheric Temperature, Density, and Composition: New Models. Special Report No. 375, Smithsonian Astrophysical Observatory, Cambridge, Massachusetts, 1977.

5. McNish, A. G., and Lincoln, J. V.: Prediction of Sunspot Numbers. Trans actions, American Geophysical Union, 30, 1949, p. 673.

6. Boykin, E. P., and Richards, T. J.: Application of the Lincoln McNish Technique to the Prediction of the Remainder of the Twentieth Sunspot Cycle. Lockheed Missiles and Space Company, Technical Memorandum 54/30-89, Huntsville, Alabama, March 1966.

7. Avaritt, D.: Sunspot Prediction Program (Sunspot Deck). Program Document 3F0360, Computer Sciences Corporation, Huntsville, Alabama, 1972.

8. Scissum, J.: Survey of Solar Cycle Prediction Models. NASA TM-55593, 1967.

9. Slutz, R. J.; Gray, T. B.; West, M. L.; Stewart, F. G.; and Leftin, Margo: Solar Activity Prediction. NASA CR-1939, November 1971.

10. Vitinskii, Yu, I.: Solar-Activity Forecasting. Translated from Russian, Israel Program for Scientific Translations, Jerusalem. NASA TT F-289, Clearing House for Federal Scientific and Technical Information, Springfield, Virginia, 1965.

11. Math Pack, Univac Data Processing Division 1108, Report No. UP 4051 Rev 1, Sperry Rand Corporation, Philadelphia, Pennsylvania, 1967.

12. Kirk, Roger E.: Introductory Statistics. Brooks/Cole Publishing Co., Monterey, California, 1978, pp. 331-335.

13. Waldmeier, M.: The Sunspot Activity in the Years 1610-1960. Zurich Schulthess and Company, Switzerland, 1961.

14. Chernosky, E. J., and Hagan, M. P.: The Zurich Sunspot Number and Its Variation for 1700-1957. J. Geophys. Res., 63, No. 4, 1958, p. 775.

15. Schove, D. Justin: The Sunspot Cycle, 649 B.C. to A.D. 2000. J. Geophys. Res., 60, No. 2, 1955, p. 127.

16. Scarbrough, J. B.: Numerical Mathematical Analysis. Johns Hopkins Press, Baltimore, Maryland, 1962, p. 133.

# APPROVAL

## LAGRANGIAN LEAST-SQUARES PREDICTION OF SOLAR ACTIVITY

By Robert L. Holland, C. A. Rhodes
and Harold C. Euler, Jr.

The information in this report has been reviewed for technical content. Review of any information concerning Department of Defense or nuclear energy activities or programs has been made by the MSFC Security Classification Officer. This report, in its entirety, has been determined to be unclassified.

GEORGE H. FICHTL
Chief, Fluid Dynamics Branch

WILLIAM W. VAUGHAN
Chief, Atmospheric Sciences Division

C. R. O'DELL
Acting Director, Space Sciences Laboratory

☆U.S. GOVERNMENT PRINTING OFFICE 1982–546-071/209 REGION NO. 7